

CASE FILE
COPY



RM A51K28

RESEARCH MEMORANDUM

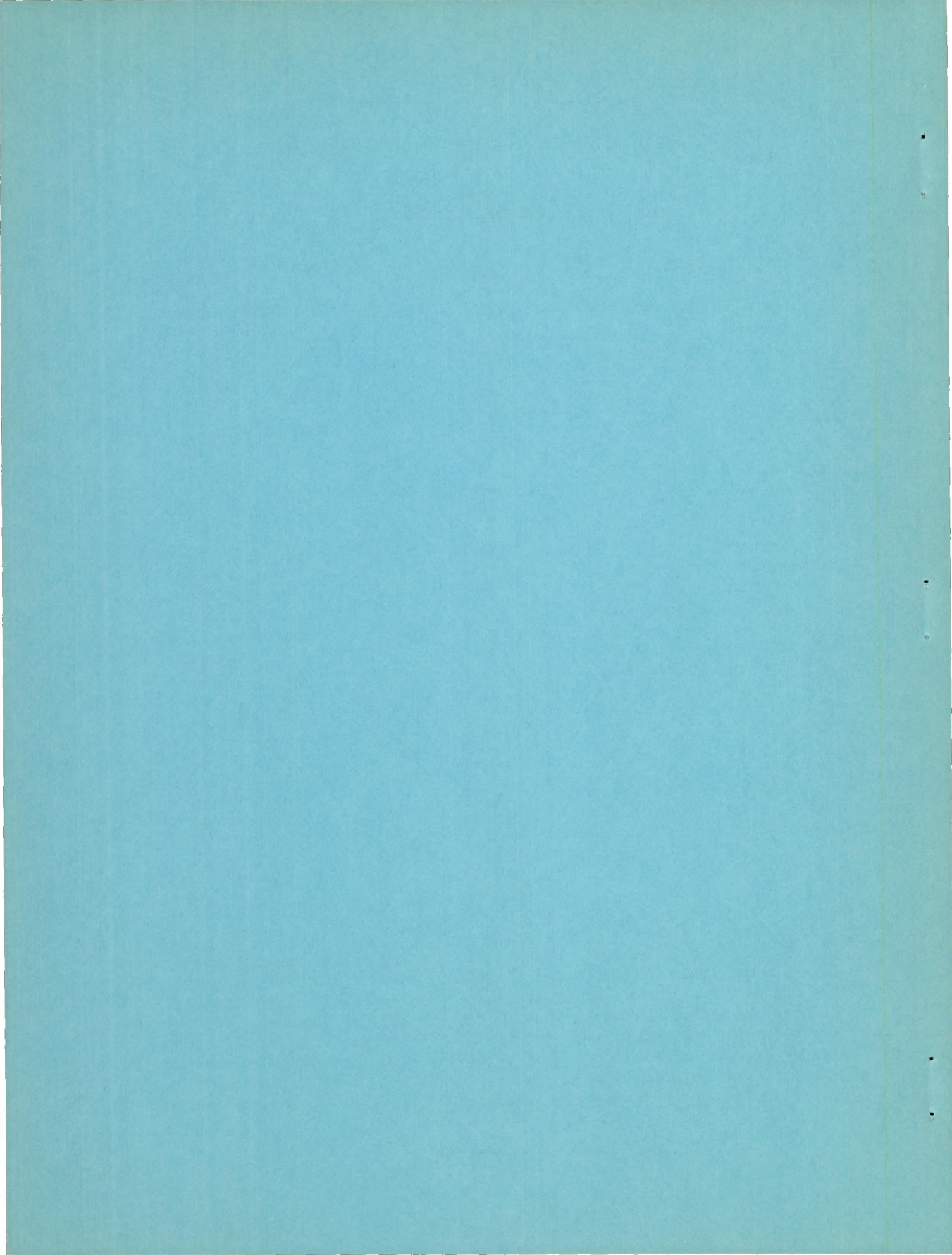
LIFT, DRAG, AND PITCHING MOMENT OF LOW-ASPECT-RATIO WINGS AT
SUBSONIC AND SUPERSONIC SPEEDS - AN INVESTIGATION AT LARGE
REYNOLDS NUMBERS OF THE LOW-SPEED CHARACTERISTICS
OF SEVERAL WING-BODY COMBINATIONS

By Donald W. Smith, Harry H. Shibata, and Ralph Selan

Ames Aeronautical Laboratory
Moffett Field, Calif.

NATIONAL ADVISORY COMMITTEE
FOR AERONAUTICS
WASHINGTON

February 15, 1952
Declassified April 8, 1957



NATIONAL ADVISORY COMMITTEE FOR AERONAUTICS

RESEARCH MEMORANDUM

LIFT, DRAG, AND PITCHING MOMENT OF LOW-ASPECT-RATIO WINGS AT
SUBSONIC AND SUPERSONIC SPEEDS - AN INVESTIGATION AT LARGE
REYNOLDS NUMBERS OF THE LOW-SPEED CHARACTERISTICS
OF SEVERAL WING-BODY COMBINATIONS

By Donald W. Smith, Harry H. Shibata, and Ralph Selan

SUMMARY

Several wing-body combinations having wings suitable for supersonic interceptor-type aircraft have been investigated at large Reynolds numbers and low Mach numbers. Nine wing-body combinations were tested having wing aspect ratios of 2, 3, and 4, and including triangular, trapezoidal, and swept-back plan forms. The lift, drag, and pitching moment of the models having wings of aspect ratio 2 are presented for Reynolds numbers from 4.9 million to 16.6 million at a constant Mach number of 0.25. The characteristics for the models having wings of aspect ratios 3 and 4 are presented for Reynolds numbers from approximately 2.4 million to 10.6 million at a constant Mach number of 0.25. A comparison of the characteristics measured in both the Ames 12-foot pressure wind tunnel and the Ames 6- by 6-foot supersonic wind tunnel at a Mach number of 0.60 and a Reynolds number of 4.9 million for the models having wings of aspect ratio 2 and approximately 2.4 million for the models having wings of aspect ratios 3 and 4 is included.

INTRODUCTION

A research program is in progress at the Ames Aeronautical Laboratory to ascertain experimentally, at subsonic and supersonic Mach numbers, the characteristics of wings of interest in the design of high-speed fighter airplanes. Variations in plan form, twist, camber, and thickness are being investigated. The results published to date in this program are presented in references 1 through 13. This report presents the low-speed, large Reynolds number characteristics of nine of the wings being investigated in this program. The characteristics of some of these nine

wings in the Mach number range from 0.60 to 1.70 have been published in reference 5 and references 7 through 12. In all cases the wings have been tested in combination with a body. As in references 1 through 13, the data are presented herein without analysis to expedite publication.

NOTATION

b wing span, feet

\bar{c} mean aerodynamic chord $\left(\frac{\int_0^{b/2} c^2 dy}{\int_0^{b/2} c dy} \right)$, feet

c local wing chord, feet

l length of body including portion removed to accommodate sting, inches

$\frac{L}{D}$ lift-drag ratio

$\left(\frac{L}{D} \right)_{max}$ maximum lift-drag ratio

M Mach number

q free-stream dynamic pressure, pounds per square foot

R Reynolds number based on mean aerodynamic chord

r radius of body, inches

r_o maximum body radius, inches

S total wing area including the area formed by extending the leading and trailing edges to the plane of symmetry, square feet

x longitudinal distance from nose of body, inches

y distance perpendicular to plane of symmetry, feet

α angle of attack of the body axis, degrees

C_D	drag coefficient $\left(\frac{\text{drag}}{qS} \right)$
C_m	pitching-moment coefficient about the 25-percent point of the wing mean aerodynamic chord $\left(\frac{\text{pitching moment}}{qS\bar{c}} \right)$
C_L	lift coefficient $\left(\frac{\text{lift}}{qS} \right)$
$\frac{dC_L}{da}$	slope of the lift curve measured at zero lift, per degree
$\frac{dC_m}{dC_L}$	slope of the pitching-moment curve measured at zero lift

APPARATUS

Wind Tunnel and Equipment

The experimental investigation was conducted in the Ames 12-foot pressure wind tunnel and in the Ames 6- by 6-foot supersonic wind tunnel. In each wind tunnel the Mach number can be varied continuously and the stagnation pressure can be regulated to maintain a given test Reynolds number. The air in these tunnels is dried to prevent formation of condensation shocks. Further information on these wind tunnels is presented in references 14 and 15.

The models were sting mounted in each tunnel, the diameter of the sting being about 73 percent of the diameter of the body base for the models having wings of aspect ratio 2.0 and about 93 percent of the diameter of the body base for the remainder of the models. The pitch plane of the model support was vertical in the 12-foot wind tunnel and horizontal in the 6- by 6-foot wind tunnel. A balance mounted on the sting support and enclosed within the bodies of the models was used to measure the aerodynamic forces and moments on the models. The balance was the 4-inch-diameter, four-component, strain-gage balance described in reference 16.

Model

Photographs of typical models mounted on the sting support in the Ames 12-foot pressure wind tunnel are shown in figure 1. The nine models had five different plan forms which are shown along with certain

model dimensions in figure 2. Other important geometric characteristics of the models are given in table I.

The wings of the models were constructed of either solid steel or by covering a solid steel spar with a tin-bismuth alloy. The body spar was also steel but was covered with aluminum to form the body contours. The surfaces of the wing and body were polished smooth.

Wings 2 and 3 were cambered and twisted to support a nearly elliptical spanwise distribution of load at a lift coefficient of 0.25 and a Mach number of 1.53. The amount of camber and twist incorporated in these wings and the method by which it was determined are presented in reference 8.

The sharp leading edges of wings 4 and 8 were made elliptical to form wings 5 and 9. The details of the section modification are described in reference 10.

The wings had neither dihedral nor incidence, and their root chords coincided with the longitudinal center line of the fuselage.

TESTS AND PROCEDURES

Range of Test Variables

The characteristics of the models as functions of angle of attack were investigated in the Ames 12-foot pressure wind tunnel for a range of Reynolds numbers from 2.57 million per foot to 8.81 million per foot, at a constant Mach number of 0.25. Data were also obtained for a Mach number of 0.60 at a Reynolds number of 2.57 million per foot in both the 12-foot wind tunnel and the 6- by 6-foot wind tunnel.

Reduction of Data

The test data have been reduced to standard NACA coefficient form. Factors which affect the accuracy of these results and the corrections applied are discussed in the following paragraphs.

Tunnel-wall interference.- Corrections to the subsonic results for the induced effects of the tunnel walls, resulting from lift on

the model, were made according to the method of reference 17. The numerical values of these corrections (which were added to the uncorrected data) were:

$$\Delta\alpha = A C_L$$

$$\Delta C_D = B C_L^2$$

<u>Wing No.</u>	12-foot wind tunnel		6- by 6-foot wind tunnel	
	A	B	A	B
1	0.27	.0046	0.93	0.0162
2	.27	.0046	.93	.0162
3	.27	.0046	.93	.0162
4	.16	.0028	.57	.0098
5	.16	.0028	.57	.0098
6	.16	.0028	.55	.0097
7	.16	.0028	.55	.0097
8	.16	.0028	.59	.0104
9	.16	.0028	.59	.0104

No corrections were made to the pitching-moment coefficients.

The effects at subsonic speeds of constriction of the flow by the tunnel walls were taken into account by the method of reference 18. The correction was calculated for conditions at 0° angle of attack and was applied throughout the angle-of-attack range. In the 6- by 6-foot wind tunnel at a Mach number of 0.60 this correction amounted to less than a 0.9 percent increase in the Mach number and in the dynamic pressure over that determined from a calibration of the wind tunnel without a model in place. At Mach numbers of 0.25 and 0.60 in the 12-foot wind tunnel this correction was so small that it was neglected.

Stream variations.- In the test region of the 12-foot wind tunnel the stream inclination, determined from tests of a wing spanning the tunnel, is less than 0.08° . The longitudinal variation of static pressure in the region of the model is less than 0.9 percent of the dynamic pressure in this region. No correction for the effect of these stream variations was made.

Tests of the models, normal and inverted, at subsonic speeds in the 6- by 6-foot supersonic wind tunnel have indicated a stream inclination of less than 0.1° and a slight stream curvature in the pitch plane. No corrections were made to the data for the effects of these stream irregularities. No measurements have been made at subsonic speeds of the stream curvature in the yaw plane. At subsonic speeds, the longitudinal variation of static pressure in the region of the model is not known accurately at present, but a preliminary survey has indicated that it is

less than 2 percent of the dynamic pressure in this region. No correction was made to the data for the effect of this pressure variation.

Support interference.- At subsonic speeds, the effects of support interference on the aerodynamic characteristics of the models are not known. For the present tailless models, it is believed that such effects consisted primarily of changes in the pressure at the base of the models. In an effort to correct at least partially for this support interference, the base pressure was measured and the drag data were adjusted to correspond to a base pressure equal to the static pressure of the free stream.

RESULTS

The results are presented in this report without analysis in order to expedite publication. The variation of lift coefficient with angle of attack and the variation of drag coefficient, pitching-moment coefficient, and lift-drag ratio with lift coefficient at a Mach number of 0.25, and at Reynolds numbers from 2.57 million per foot to 8.81 million per foot, are shown in figures 3 through 11. There are presented in figures 12 through 20 data obtained in both the 6- by 6-foot wind tunnel and the 12-foot wind tunnel for the same models. These data were obtained at a Mach number of 0.60 and a Reynolds number of 2.57 million per foot. The results presented in figures 3 through 11 have been summarized in figures 21 and 22 to show some important parameters as functions of Reynolds number. The slope parameters have been measured at zero lift.

Ames Aeronautical Laboratory,
National Advisory Committee for Aeronautics,
Moffett Field, Calif.

REFERENCES

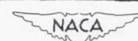
1. Smith, Donald W., and Heitmeyer, John C.: Lift, Drag, and Pitching Moment of Low-Aspect-Ratio Wings at Subsonic and Supersonic Speeds - Plane Triangular Wing of Aspect Ratio 2 With NACA 0008-63 Section. NACA RM A50K20, 1951.

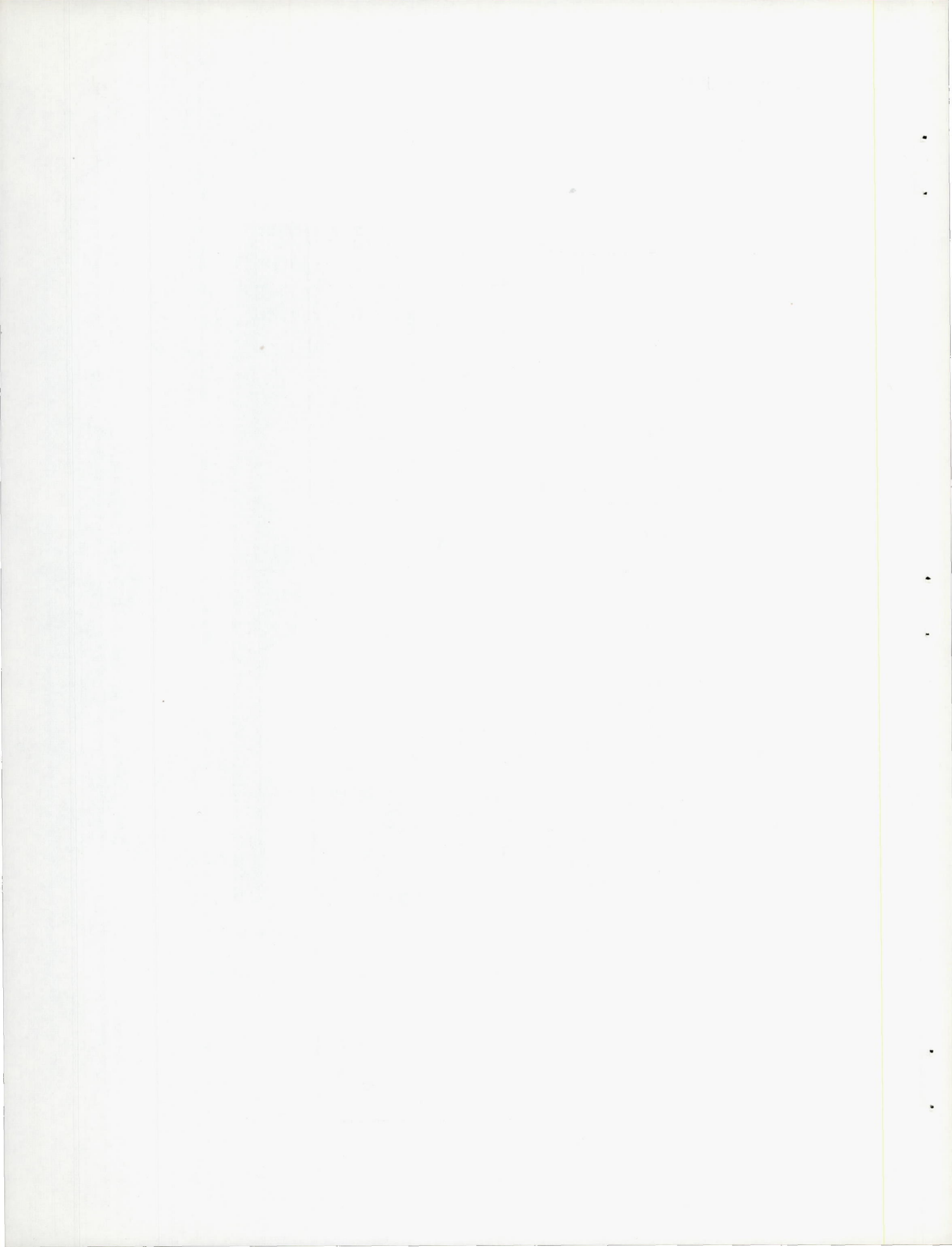
2. Smith, Donald W., and Heitmeyer, John C.: Lift, Drag, and Pitching Moment of Low-Aspect-Ratio Wings at Subsonic and Supersonic Speeds - Plane Triangular Wing of Aspect Ratio 2 With NACA 0005-63 Section. NACA RM A50K21, 1951.
3. Heitmeyer, John C., and Stephenson, Jack D.: Lift, Drag, and Pitching Moment of Low-Aspect-Ratio Wings at Subsonic and Supersonic Speeds - Plane Triangular Wing of Aspect Ratio 4 With NACA 0005-63 Section. NACA RM A50K24, 1951.
4. Phelps, E. Ray, and Smith, Willard G.: Lift, Drag, and Pitching Moment of Low-Aspect-Ratio Wings at Subsonic and Supersonic Speeds - Triangular Wing of Aspect Ratio 4 With NACA 0005-63 Thickness Distribution, Cambered and Twisted for Trapezoidal Span Load Distribution. NACA RM A50K24b, 1951.
5. Heitmeyer, John C., and Smith, Willard G.: Lift, Drag, and Pitching Moment of Low-Aspect-Ratio Wings at Subsonic and Supersonic Speeds - Plane Triangular Wing of Aspect Ratio 2 With NACA 0003-63 Section. NACA RM A50K24a, 1951.
6. Smith, Willard G., and Phelps, E. Ray: Lift, Drag, and Pitching Moment of Low-Aspect-Ratio Wings at Subsonic and Supersonic Speeds - Triangular Wing of Aspect Ratio 2 With NACA 0005-63 Thickness Distribution, Cambered and Twisted for a Trapezoidal Span Load Distribution. NACA RM A50K27a, 1951.
7. Reese, David E., Jr., and Phelps, E. Ray: Lift, Drag, and Pitching Moment of Low-Aspect-Ratio Wings at Subsonic and Supersonic Speeds - Plane Tapered Wing of Aspect Ratio 3.1 With 3-Percent-Thick, Biconvex Section. NACA RM A50K28, 1951.
8. Hall, Charles F., and Heitmeyer, John C.: Lift, Drag, and Pitching Moment of Low-Aspect-Ratio Wings at Subsonic and Supersonic Speeds - Twisted and Cambered Triangular Wing of Aspect Ratio 2 With NACA 0003-63 Thickness Distribution. NACA RM A51E01, 1951.
9. Heitmeyer, John C.: Lift, Drag, and Pitching Moment of Low-Aspect-Ratio Wings at Subsonic and Supersonic Speeds - Plane Triangular Wing of Aspect Ratio 4 With 3-Percent-Thick, Biconvex Section. NACA RM A51D30, 1951.
10. Heitmeyer, John C., and Hightower, Ronald C.: Lift, Drag, and Pitching Moment of Low-Aspect-Ratio Wings at Subsonic and Supersonic Speeds - Plane Triangular Wing of Aspect Ratio 4 With 3-Percent-Thick Rounded Nose Section. NACA RM A51F21, 1951.

11. Heitmeyer, John C.: Lift, Drag, and Pitching Moment of Low-Aspect-Ratio Wings at Subsonic and Supersonic Speeds - Plane Triangular Wing of Aspect Ratio 3 With NACA 0003-63 Section. NACA RM A51H02, 1951.
12. Heitmeyer, John C.: Lift, Drag, and Pitching Moment of Low-Aspect-Ratio Wings at Subsonic and Supersonic Speeds - Plane 45° Swept-Back Wing of Aspect Ratio 3, Taper Ratio 0.4 With 3-Percent-Thick, Biconvex Section. NACA RM A51H10, 1951.
13. Heitmeyer, John C.: Lift, Drag, and Pitching Moment of Low-Aspect-Ratio Wings at Subsonic and Supersonic Speeds - Body of Revolution. NACA RM A51H22, 1951.
14. Edwards, George G., and Stephenson, Jack D.: Tests of a Triangular Wing of Aspect Ratio 2 in the Ames 12-Foot Pressure Wind Tunnel. I - The Effect of Reynolds Number and Mach Number on the Aerodynamic Characteristics of the Wing with Flap Undeflected. NACA RM A7K05, 1948.
15. Frick, Charles W., and Olson, Robert N.: Flow Studies in the Asymmetric Adjustable Nozzle of the Ames 6- by 6-Foot Supersonic Wind Tunnel. NACA RM A9E24, 1949.
16. Olson, Robert N., and Mead, Merrill H.: Aerodynamic Study of a Wing-Fuselage Combination Employing a Wing Swept Back 63° .- Effectiveness of an Elevon as a Longitudinal Control and the Effects of Camber and Twist on the Maximum Lift-Drag Ratio at Supersonic Speeds. NACA RM A50A31a, 1950.
17. Glauert, H.: The Elements of Aerofoil and Airscrew Theory. The University Press, Cambridge, England, 1926, ch. XIV.
18. Herriot, John G.: Blockage Corrections for Three-Dimensional-Flow Closed-Throat Wind Tunnels, With Consideration of the Effect of Compressibility. NACA Rep. 995, 1950. (Formerly NACA RM A7B28)

TABLE I.- GEOMETRIC CHARACTERISTICS OF THE MODELS

Wing number	1	2	3	4	5	6	7	8	9
Aspect ratio	2	2	2	3	3	3	3	4	4
Taper ratio	0	0	0	0.4	0.4	0	0.4	0	0
Thickness distribution (streamwise)	NACA 0003-63	NACA 0005-63	NACA 0003-63	3 percent thick, biconvex	3 percent thick, biconvex, elliptic leading edge	NACA 0003-63	3 percent thick, biconvex	3 percent thick, biconvex	3 percent thick, biconvex, elliptic leading edge
Camber	none	Ref. 8	Ref. 8	none	none	none	none	none	none
Twist, degrees	0	Ref. 8	Ref. 8	0	0	0	0	0	0
Total area, S, square feet	4.014	4.014	4.014	2.425	2.425	2.430	2.431	2.425	2.425
Mean aerodynamic chord, \bar{c} , feet	1.889	1.889	1.889	0.943	0.943	1.199	0.955	1.038	1.038







(a) Wing of aspect ratio 3 mounted on the small body.

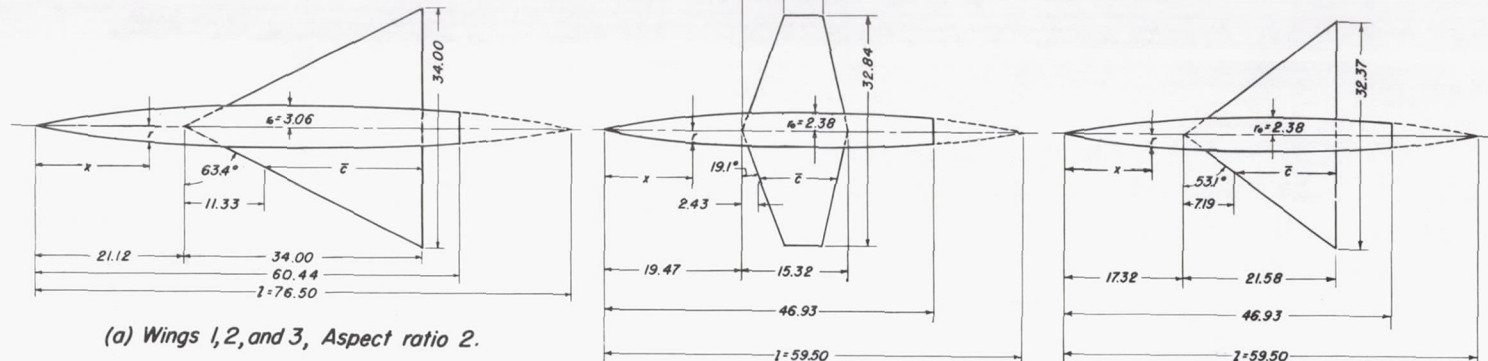
Figure 1.— Models mounted in the 12-foot wind tunnel.



NACA
A-16458

(b) Wing of aspect ratio 2 mounted on the large body.

Figure 1.- Concluded.



Equation of fuselage ordinates:

$$\frac{r}{l_0} = \left[1 - \left(1 - \frac{2x}{l} \right)^2 \right]^{\frac{3}{4}}$$

All dimensions shown in inches
unless otherwise noted

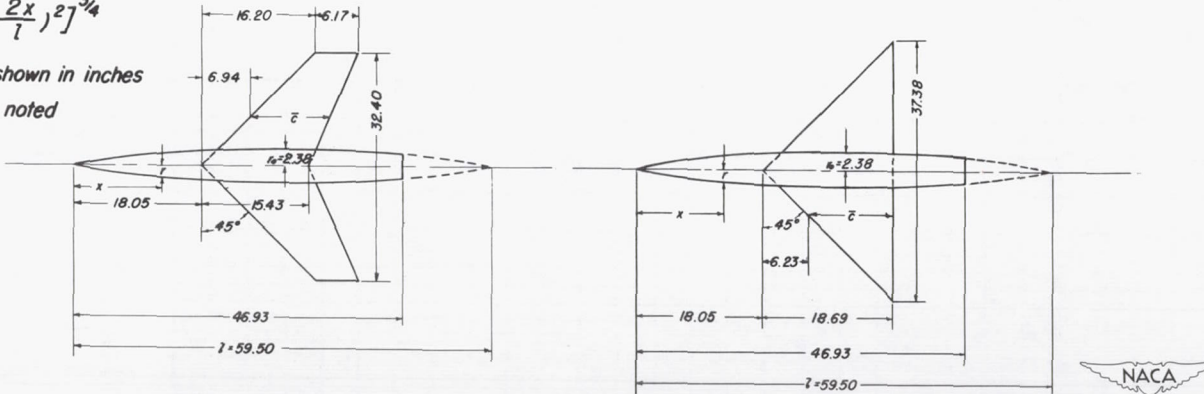


Figure 2.-Plan view of the models.

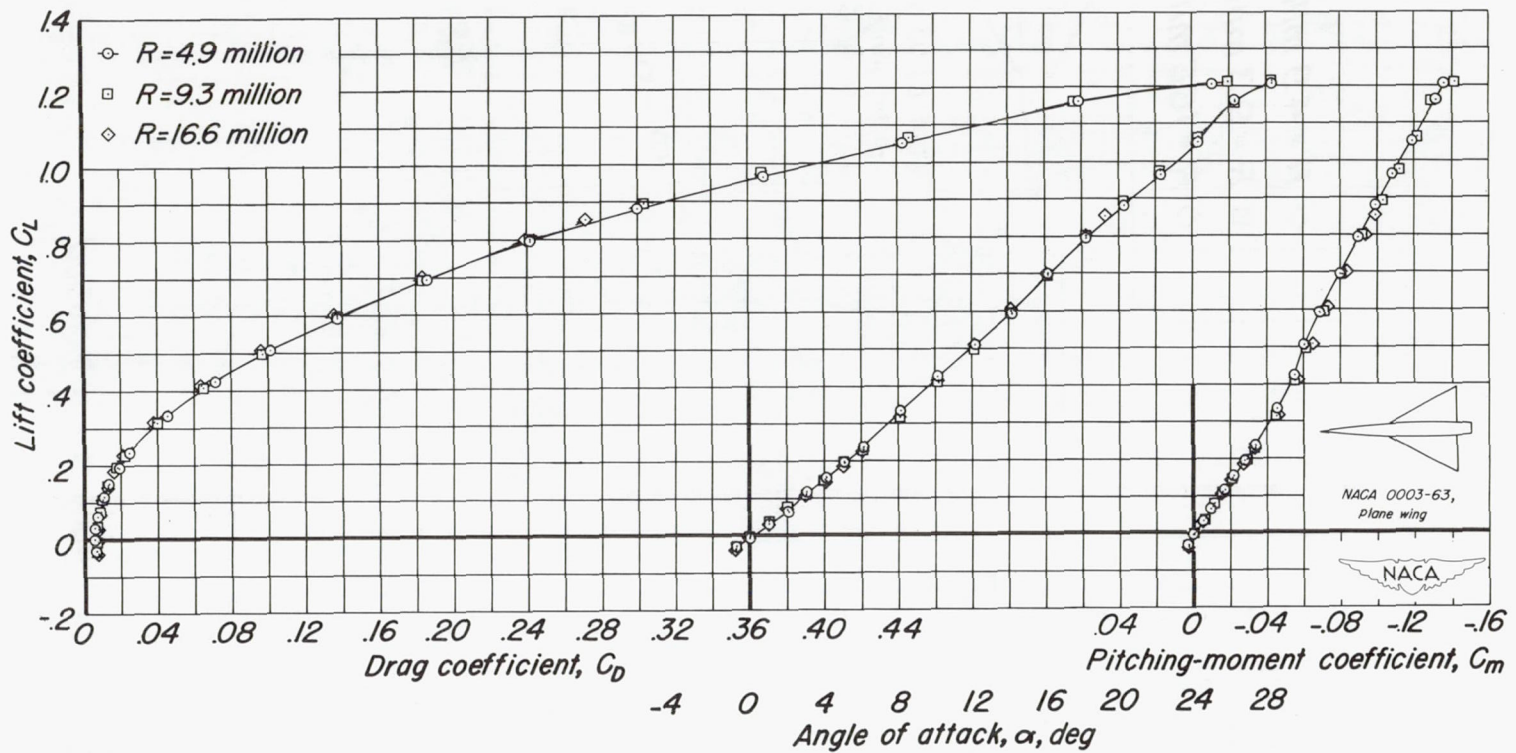
(a) C_L vs C_D , C_L vs α , C_L vs C_m

Figure 3.-The variation of the aerodynamic characteristics with lift coefficient for wing number 1 at various Reynolds numbers. $M, 0.25$.

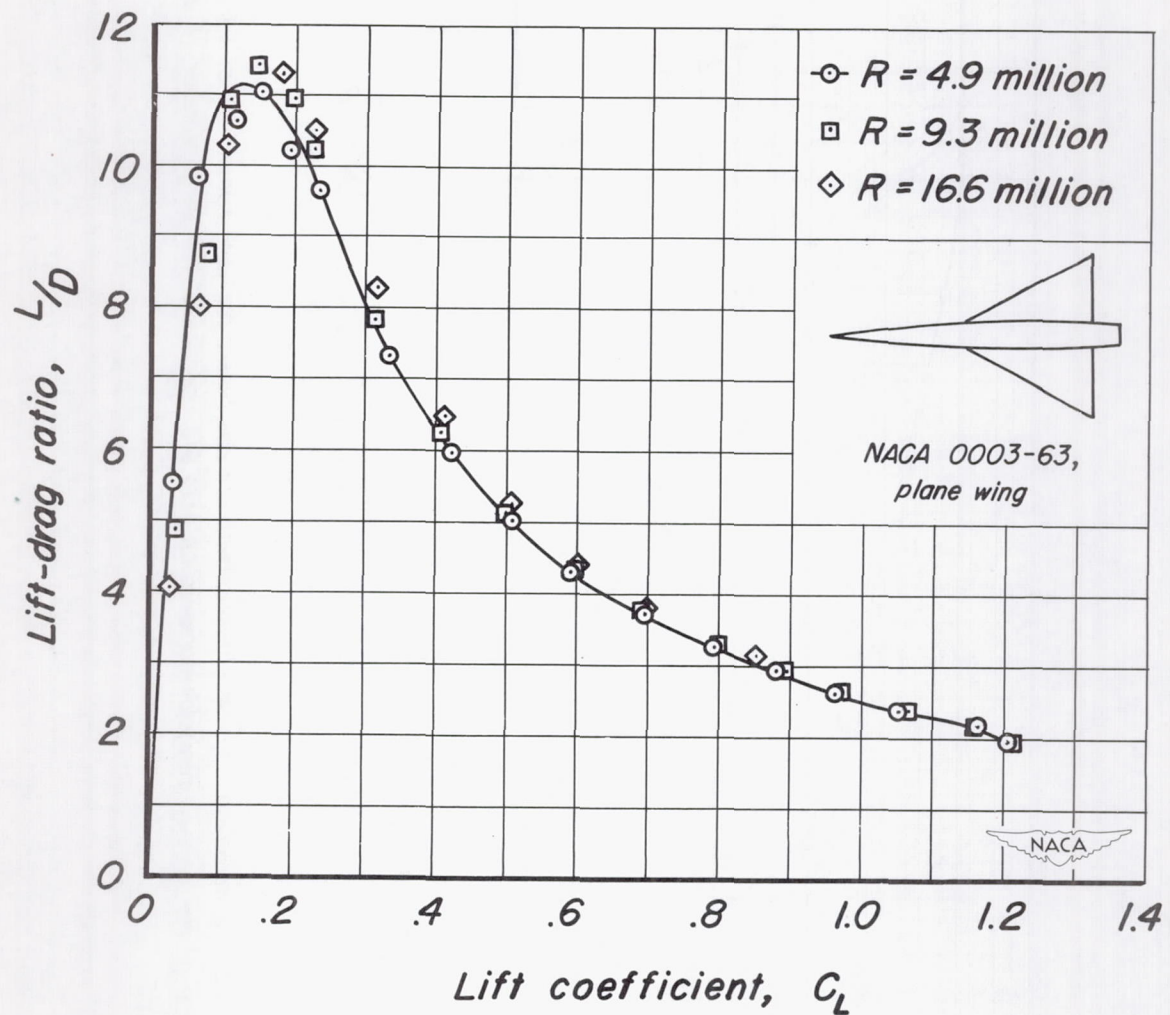
(b) L/D vs C_L

Figure 3.-Concluded.

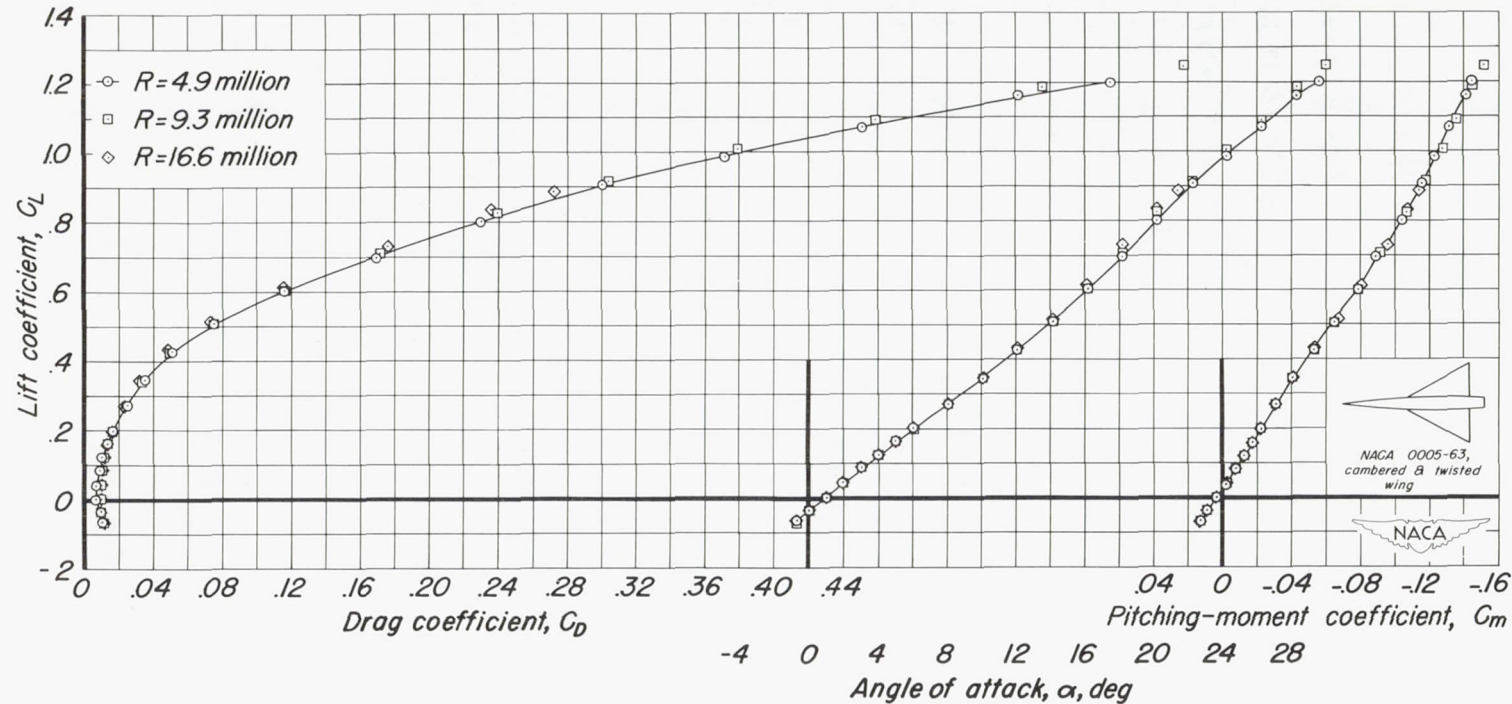
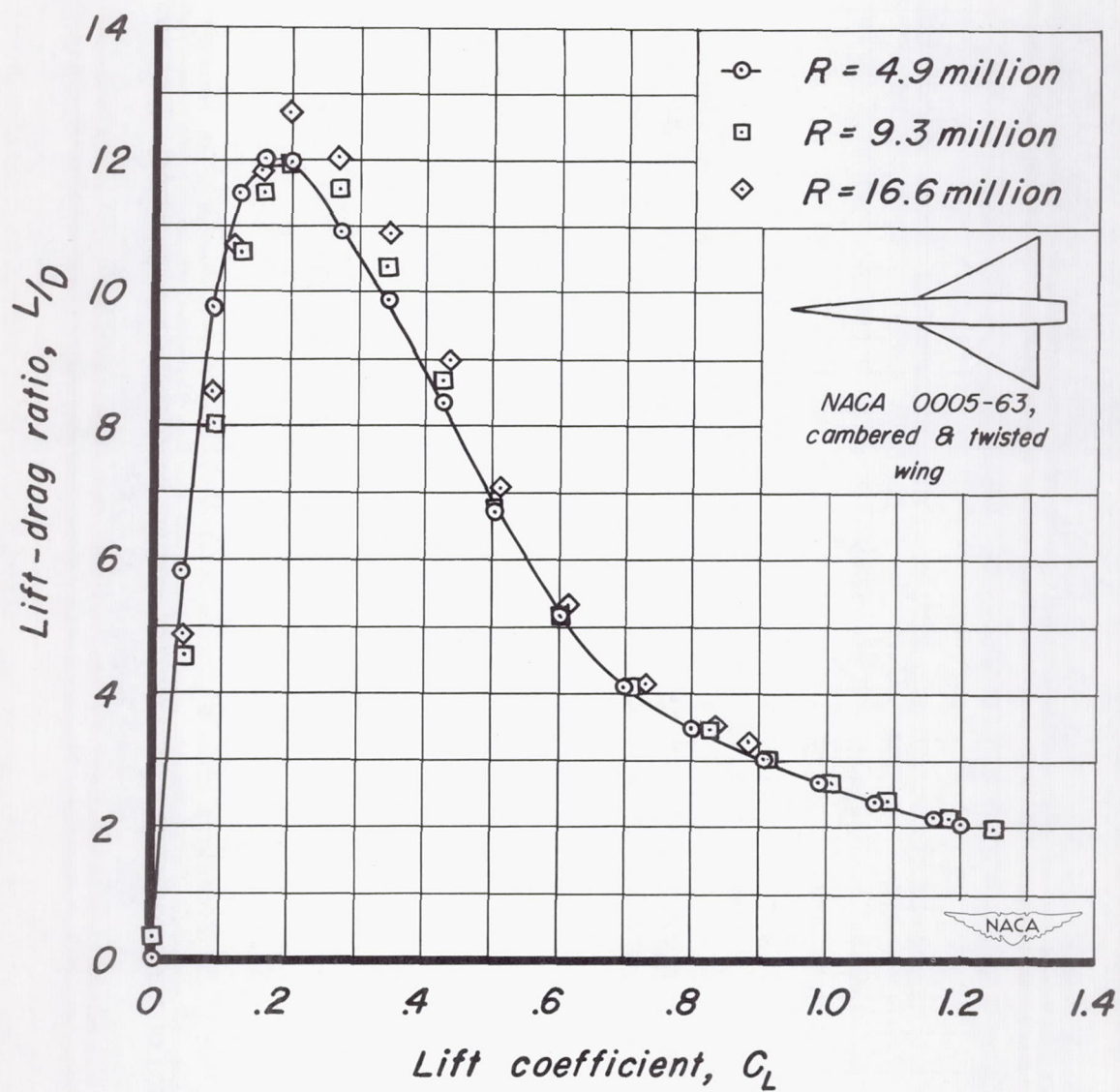
(a) C_L vs C_D , C_L vs α , C_L vs C_m

Figure 4.-The variation of the aerodynamic characteristics with lift coefficient for wing number 2 at various Reynolds numbers. $M, 0.25$.



(b) L/D vs C_L

Figure 4.-Concluded.

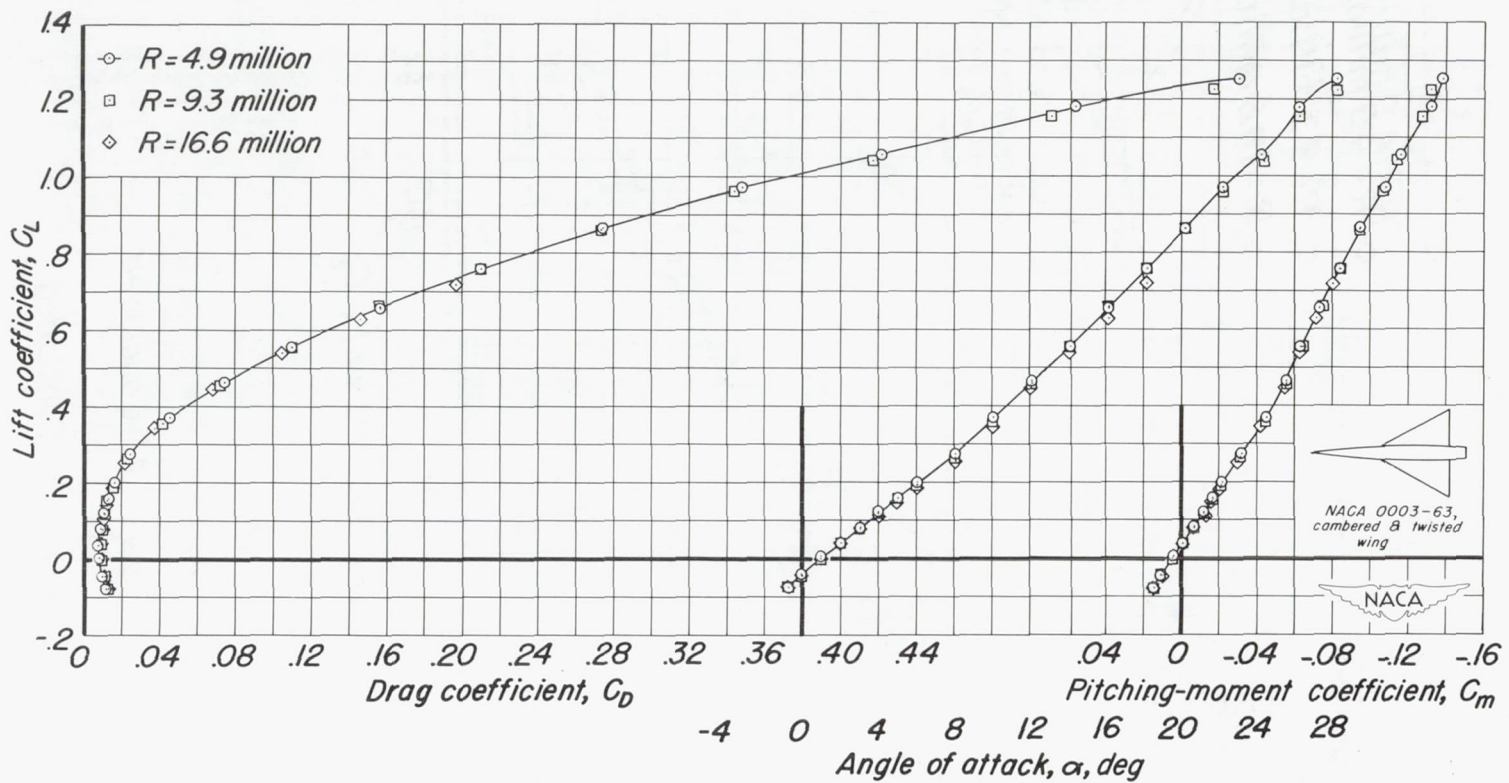
(a) C_L vs C_D , C_L vs α , C_L vs C_m

Figure 5.-The variation of the aerodynamic characteristics with lift coefficient for wing number 3 at various Reynolds numbers. $M, 0.25$.

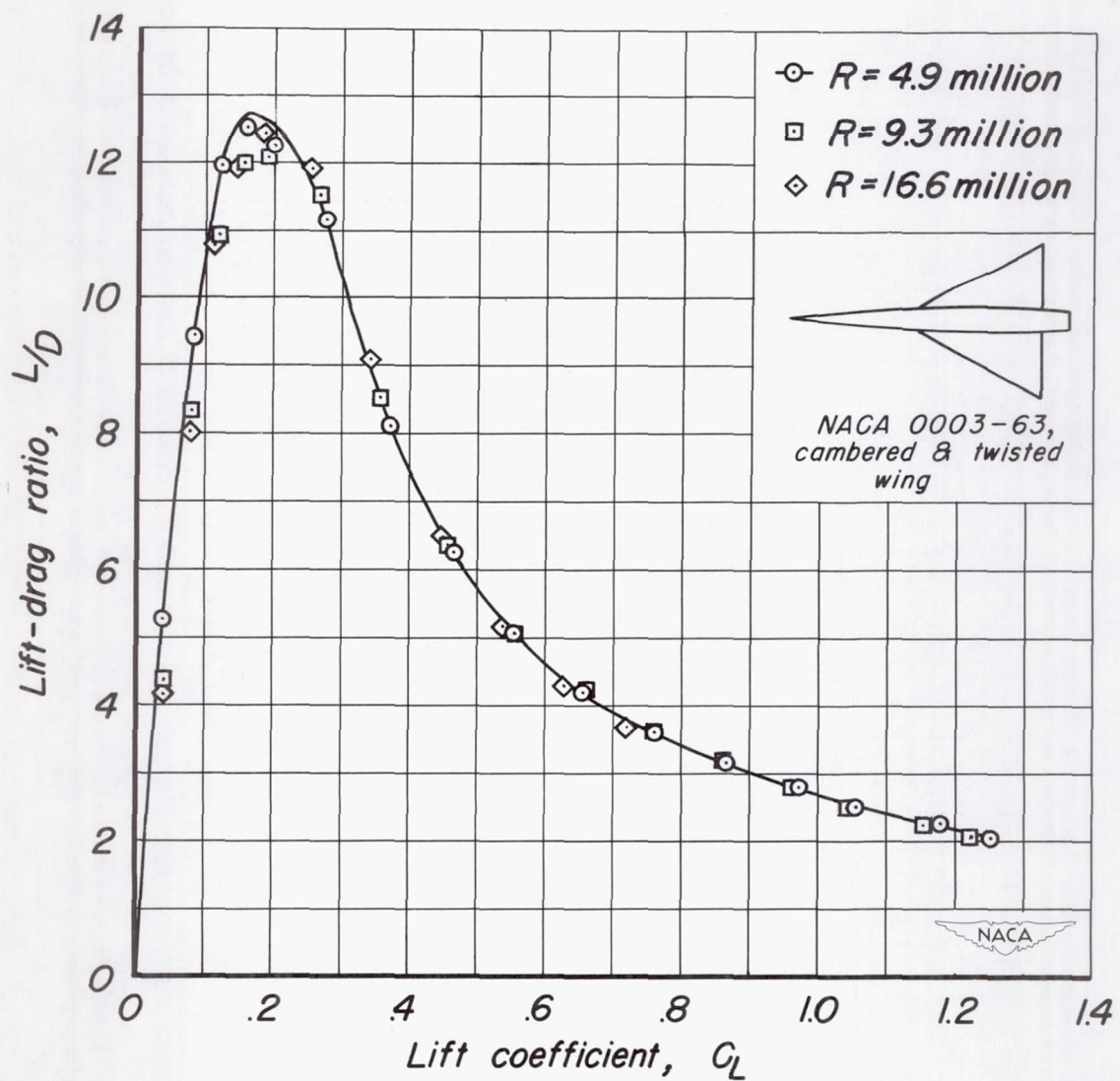
(b) L/D vs C_L

Figure 5 .-Concluded.

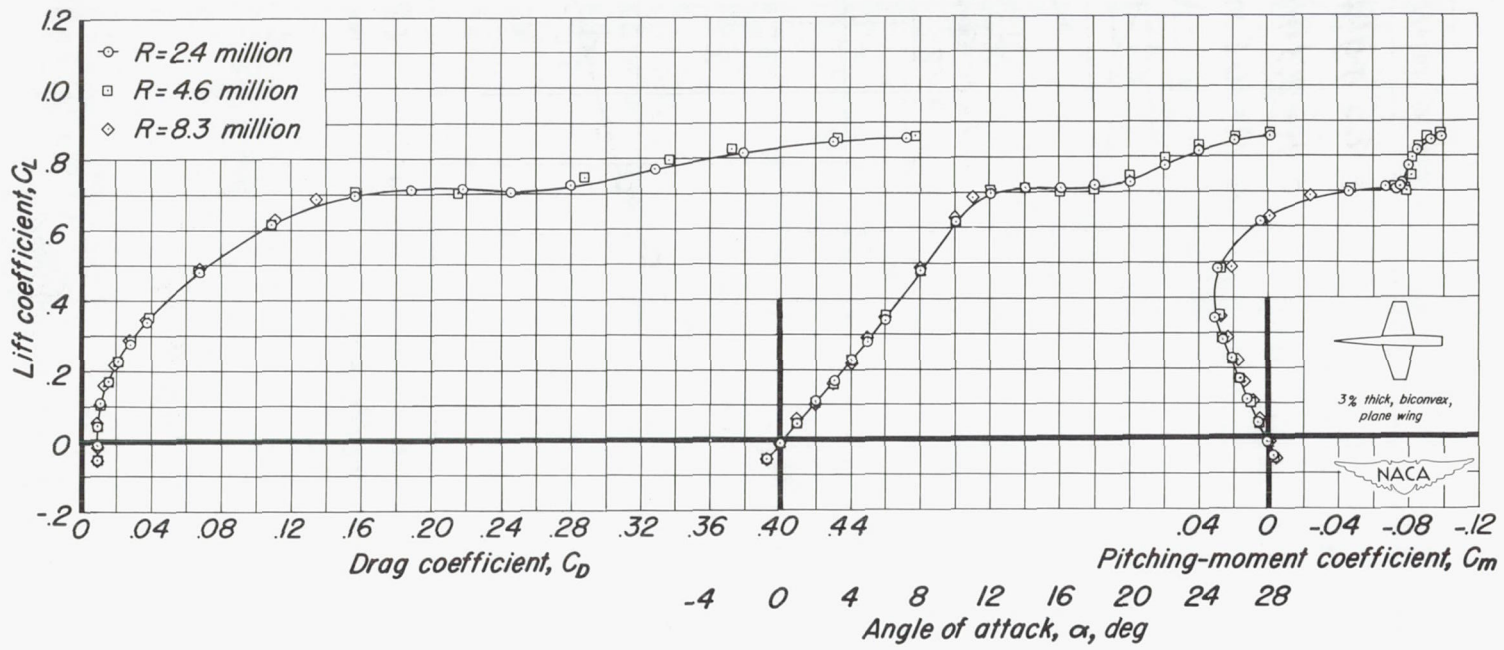
(a) C_L vs C_D , C_L vs α , C_L vs C_m

Figure 6.-The variation of the aerodynamic characteristics with lift coefficient for wing number 4 at various Reynolds numbers. $M, 0.25$.

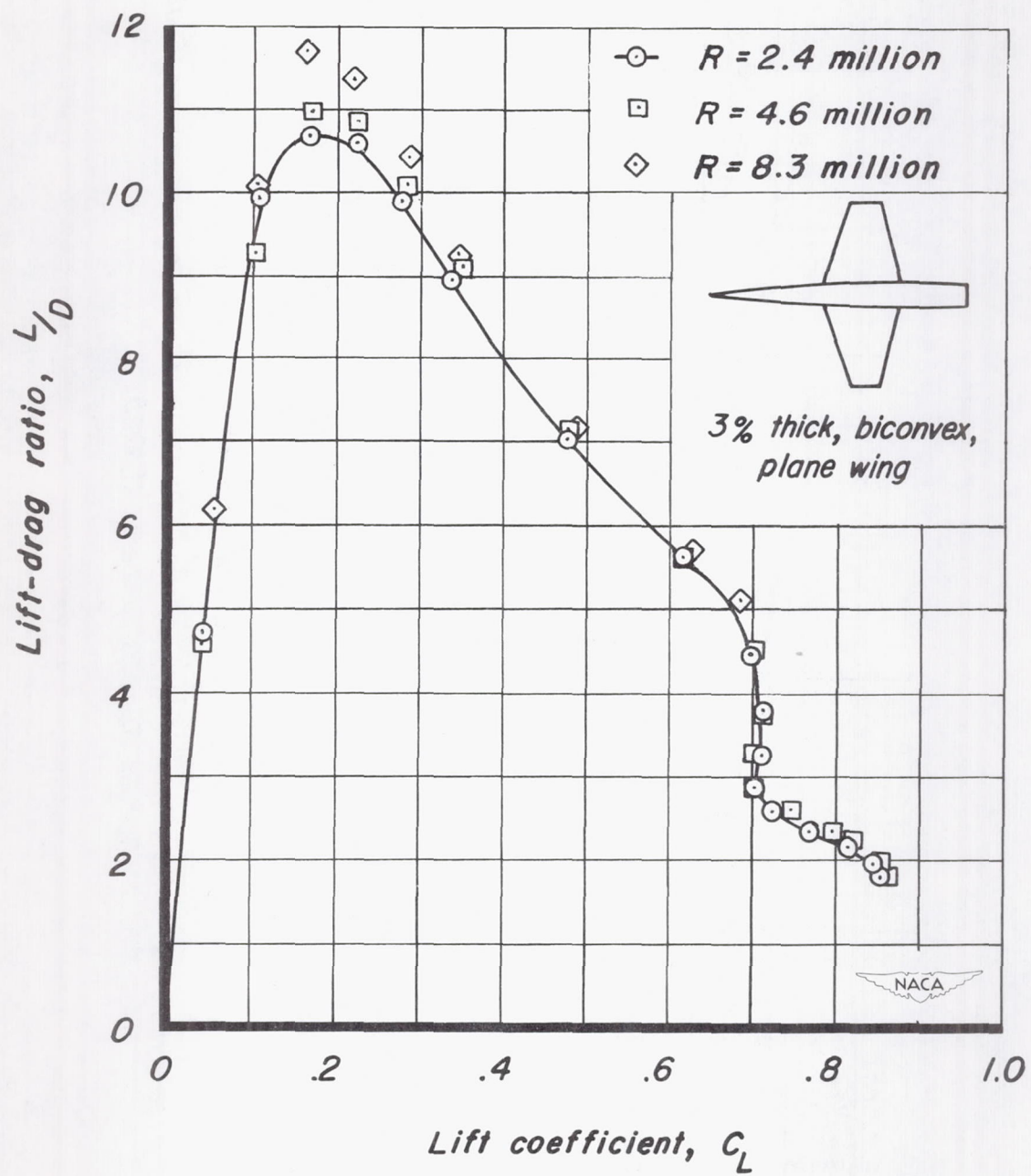
(b) L/D vs C_L

Figure 6 - Concluded.

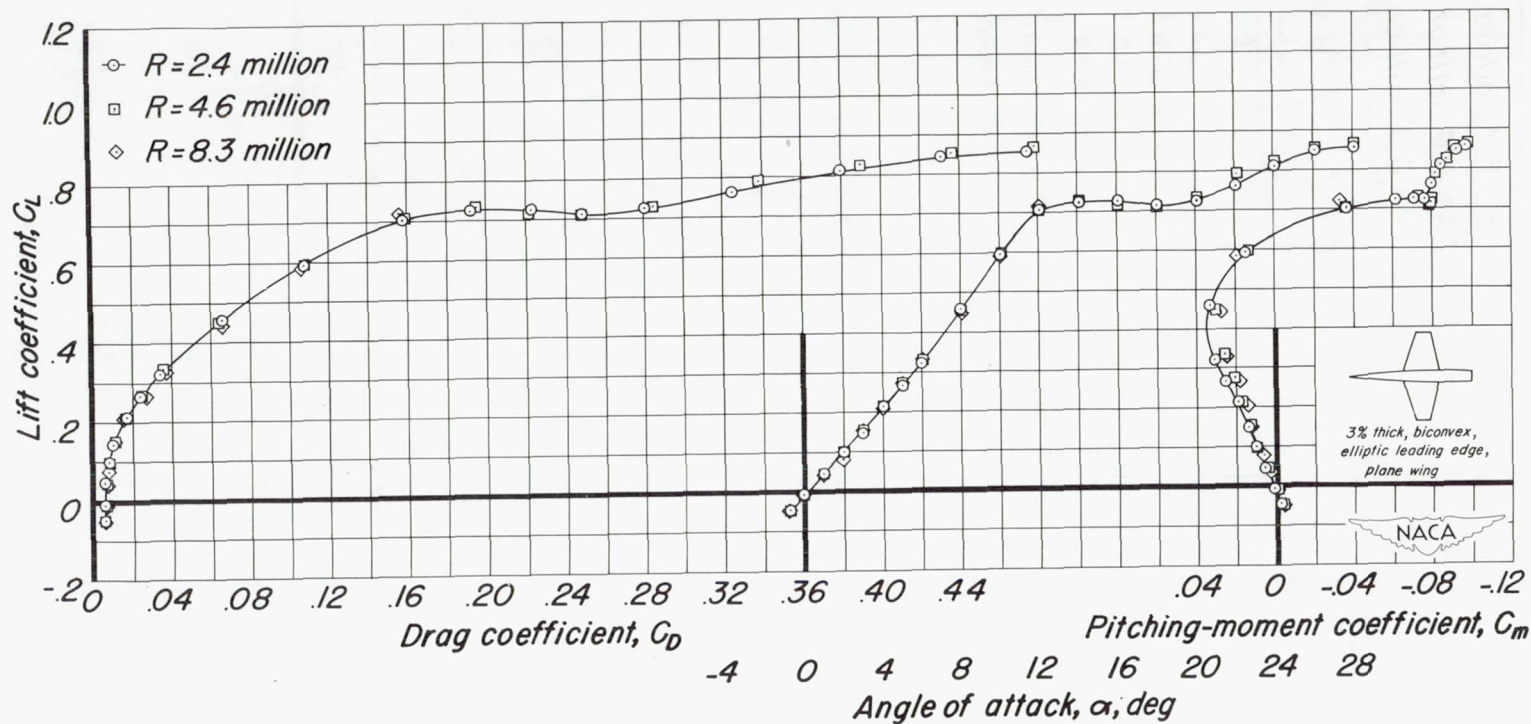
(a) C_L vs C_D , C_L vs α , C_L vs C_m

Figure 7.—The variation of the aerodynamic characteristics with lift coefficient for wing number 5 at various Reynolds numbers. $M, 0.25$.

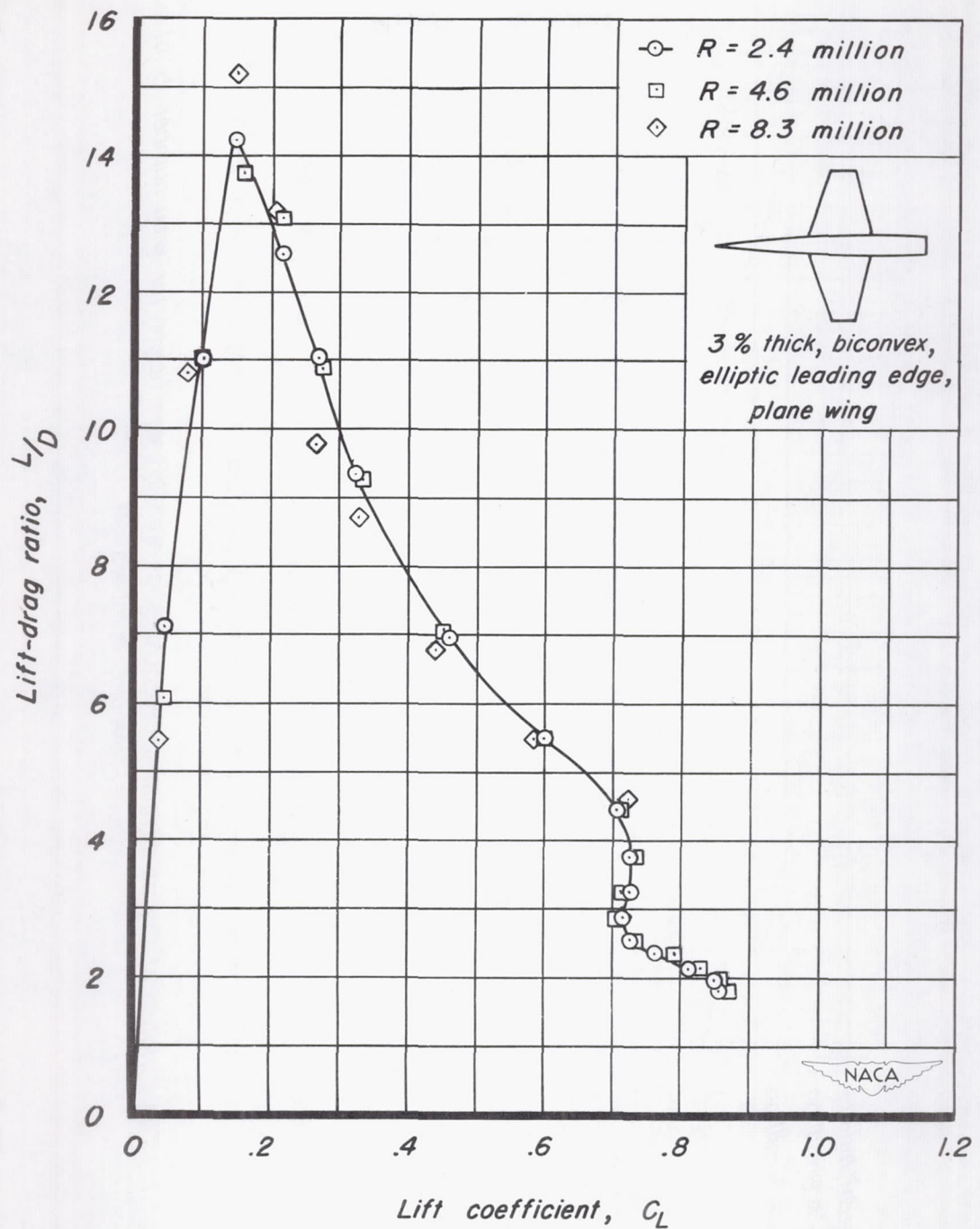
(b) L/D vs C_L

Figure 7.-Concluded.

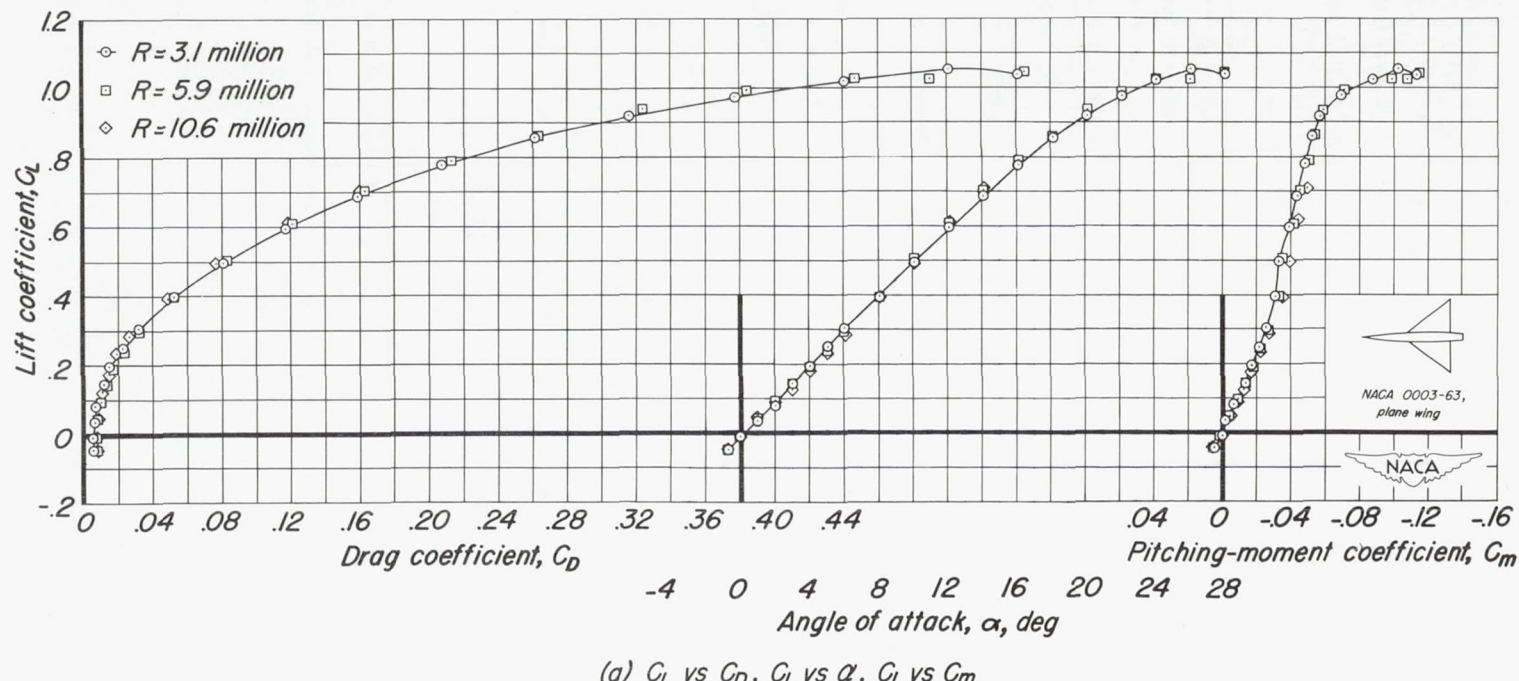


Figure 8.-The variation of the aerodynamic characteristics with lift coefficient for wing number 6 at various Reynolds numbers. $M, 0.25$.

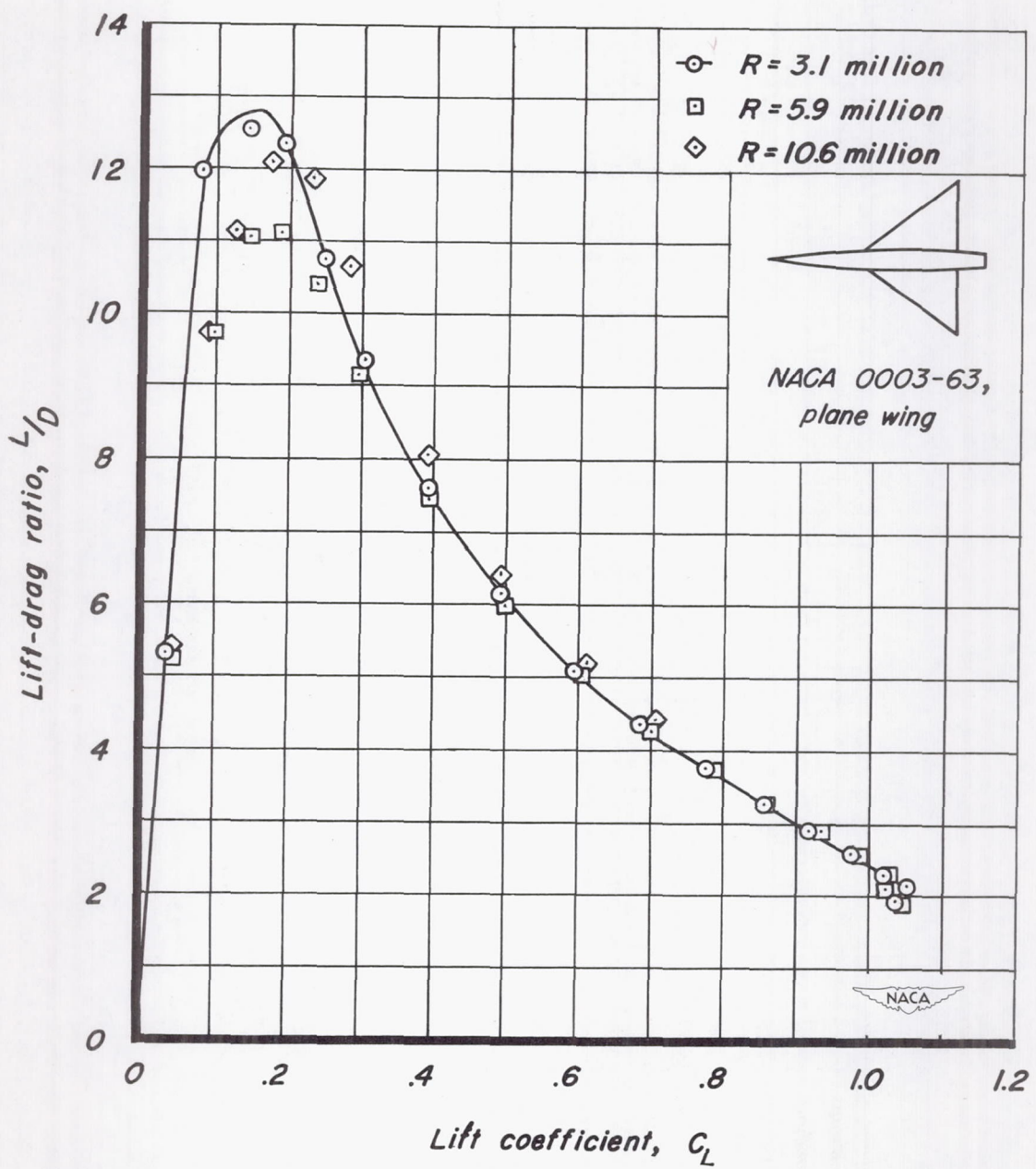
(b) L/D vs C_L

Figure 8.-Concluded.

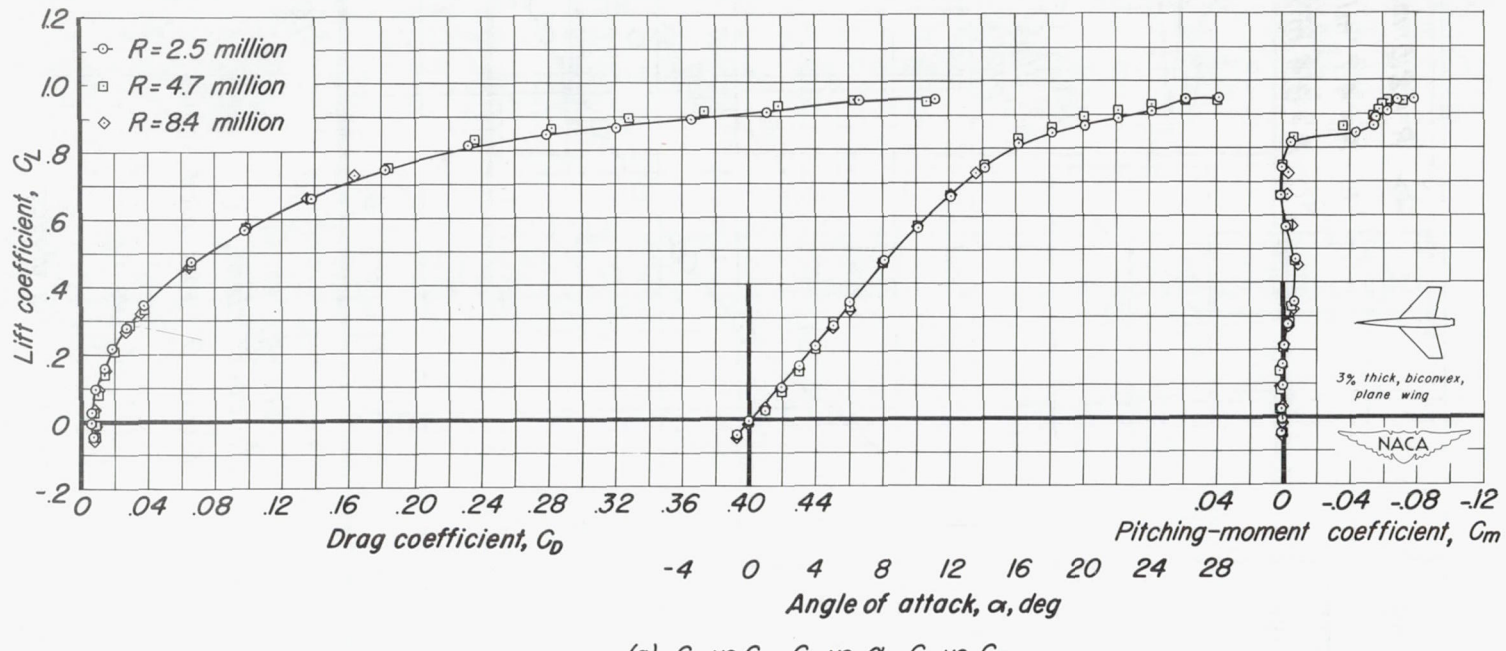


Figure 9.-The variation of the aerodynamic characteristics with lift coefficient for wing number 7 at various Reynolds numbers. $M, 0.25$.

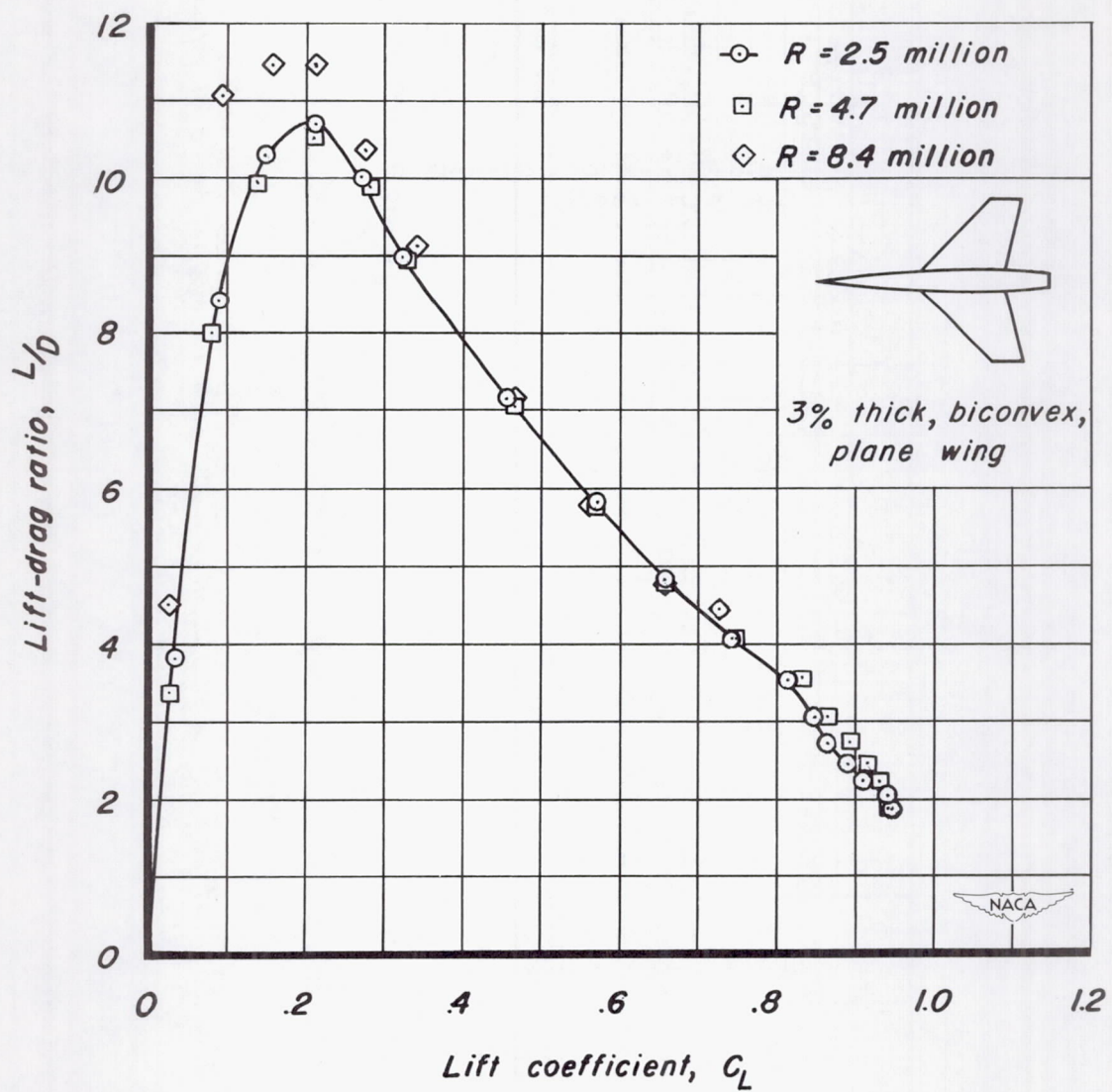
(b) L/D vs C_L

Figure 9.-Concluded.

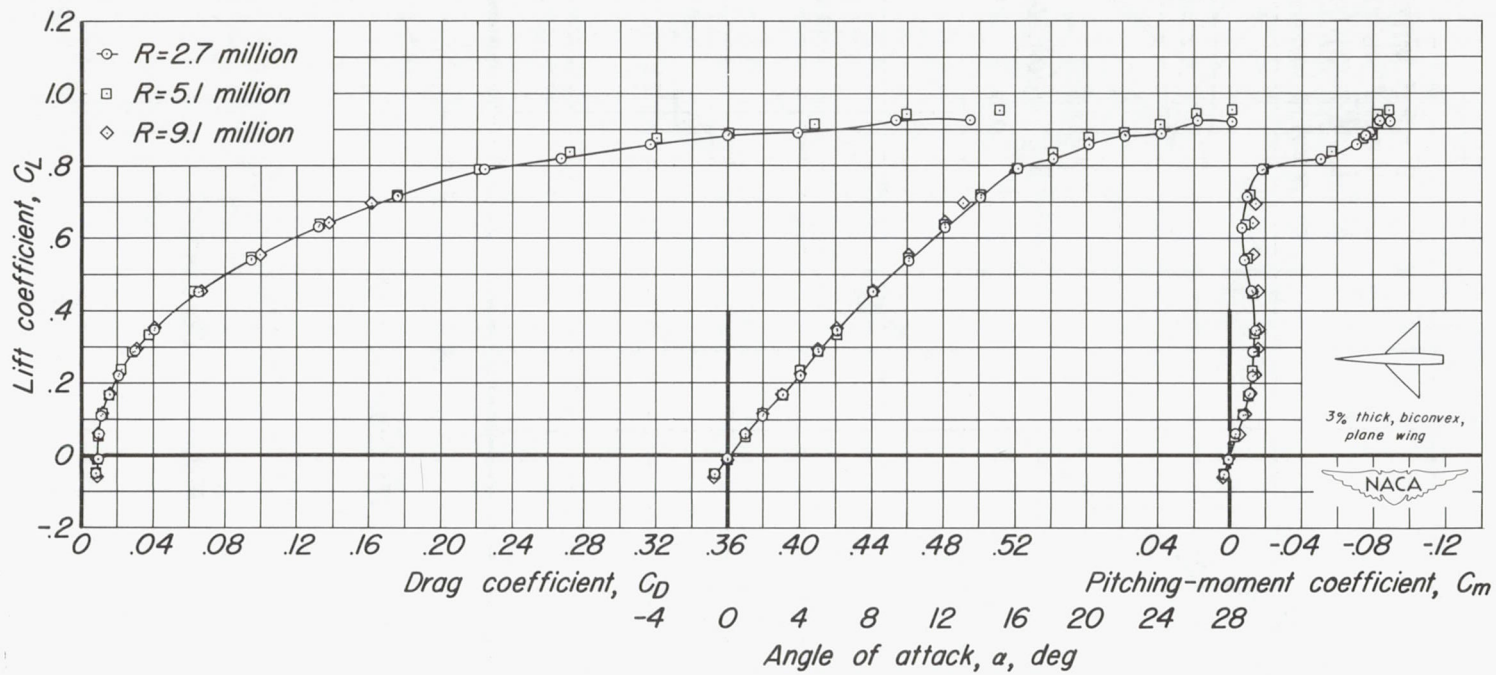
(a) C_L vs C_D , C_L vs α , C_L vs C_m

Figure 10.-The variation of the aerodynamic characteristics with lift coefficient for wing number 8 at various Reynolds numbers. $M, 0.25$.

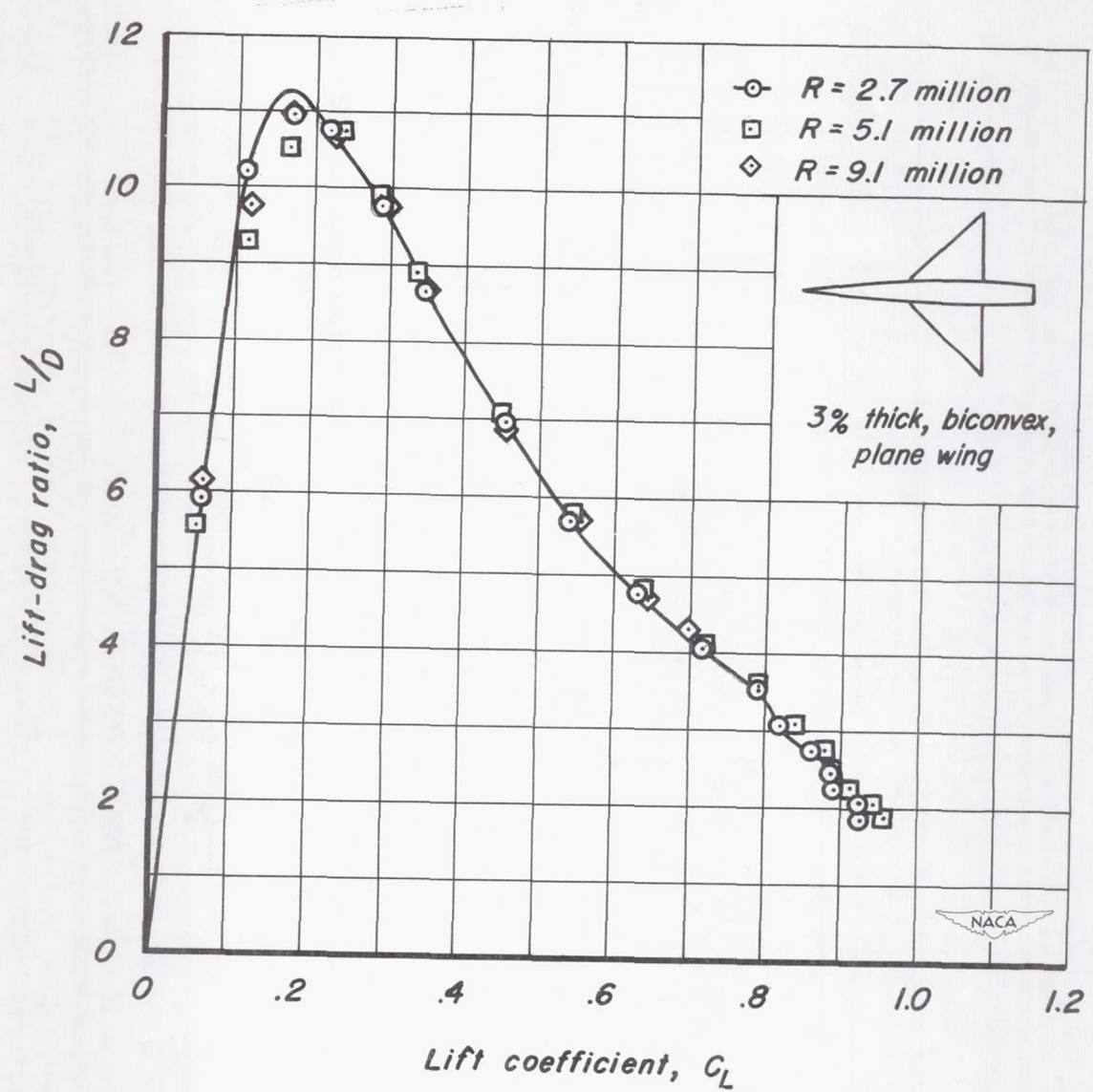
(b) L/D vs C_L

Figure 10.-Concluded.

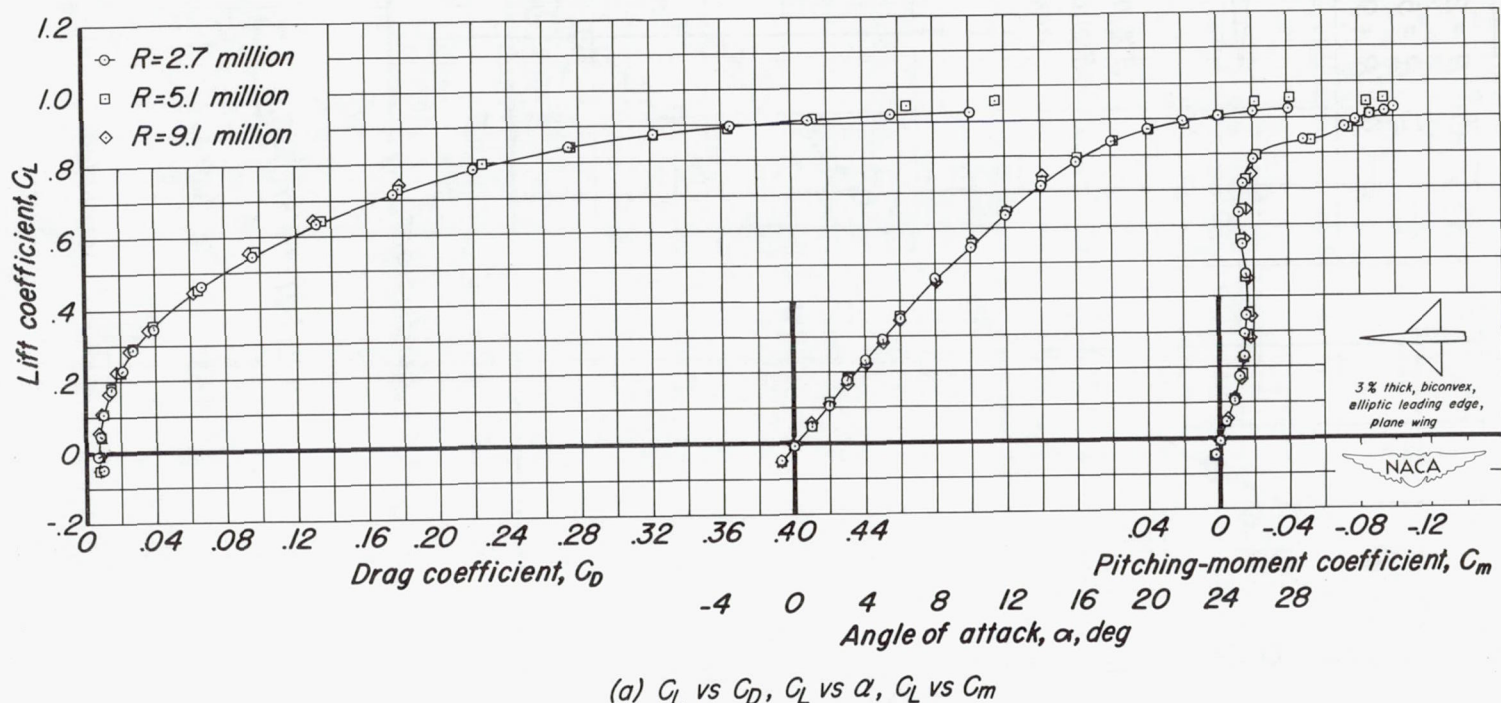


Figure 11.-The variation of the aerodynamic characteristics with lift coefficient for wing number 9 at various Reynolds numbers. $M, 0.25$.

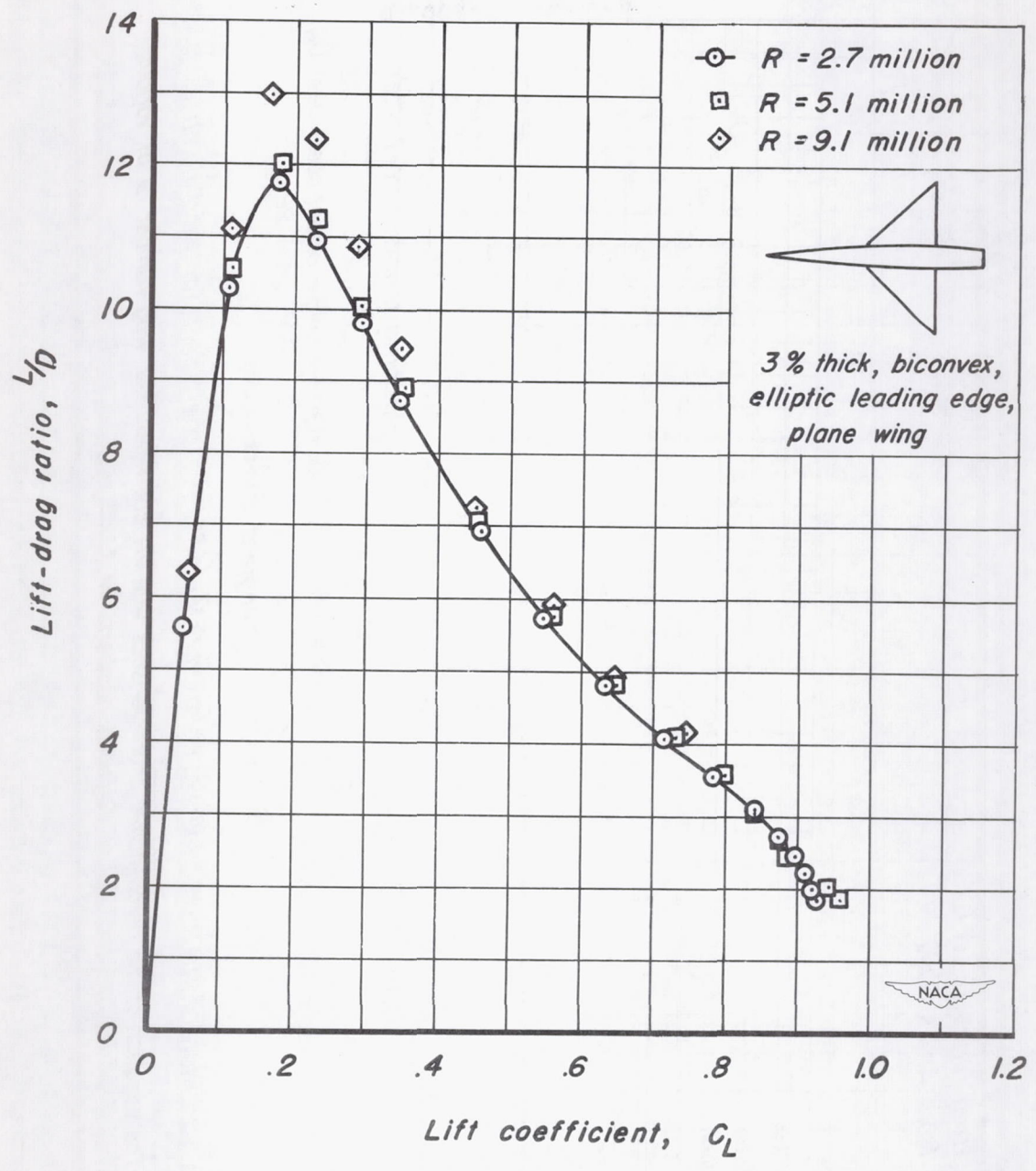
(b) L/D vs C_L

Figure 11.-Concluded.

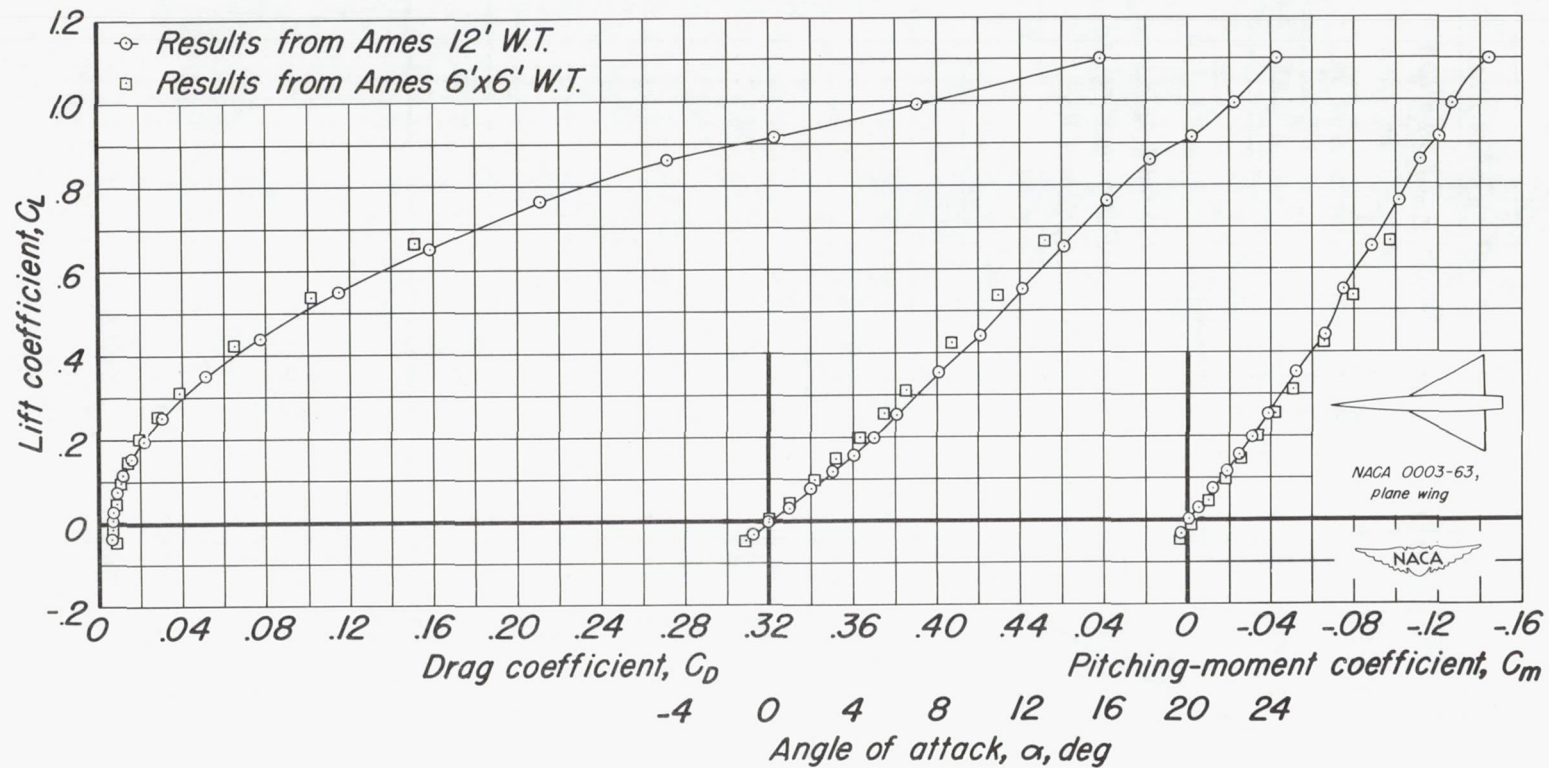
(a) C_L vs C_D , C_L vs α , C_L vs C_m

Figure 12.-The variation of the aerodynamic characteristics with lift coefficient for wing number 1 at a Mach number of 0.60. R , 4.9 million.

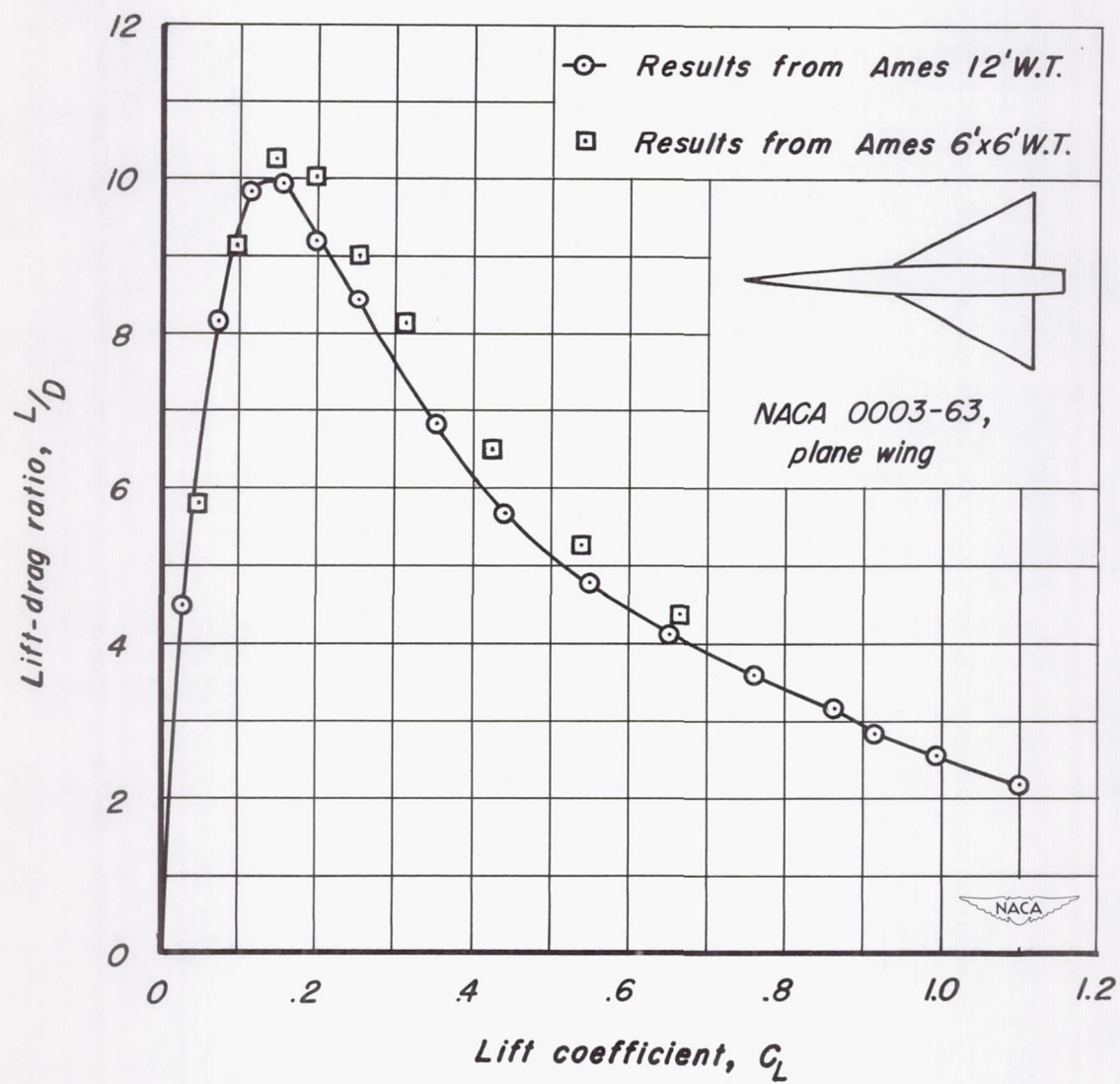
(b) L/D vs C_L

Figure 12-Concluded.

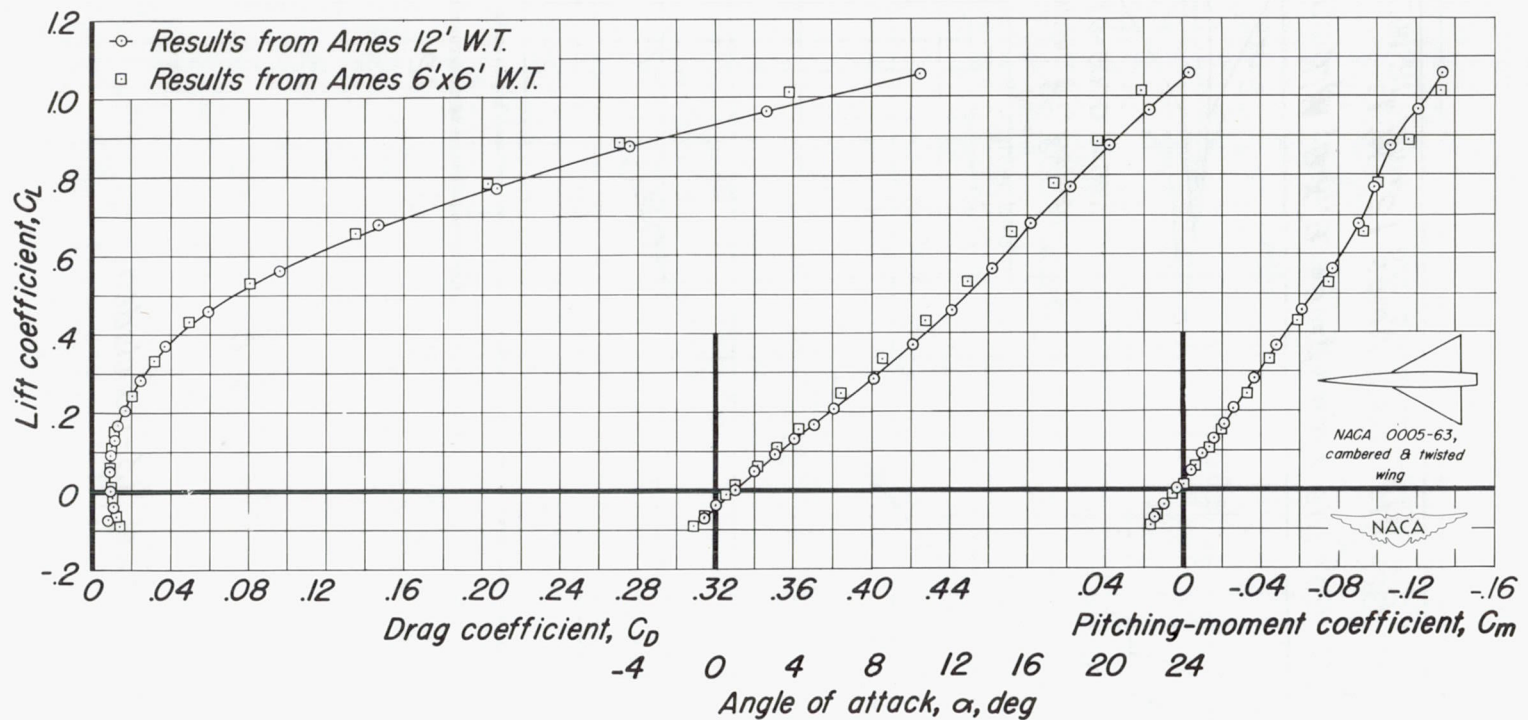
(a) C_L vs C_D , C_L vs α , C_L vs C_m

Figure 13.-The variation of the aerodynamic characteristics with lift coefficient for wing number 2 at a Mach number of 0.60. R , 4.9 million.

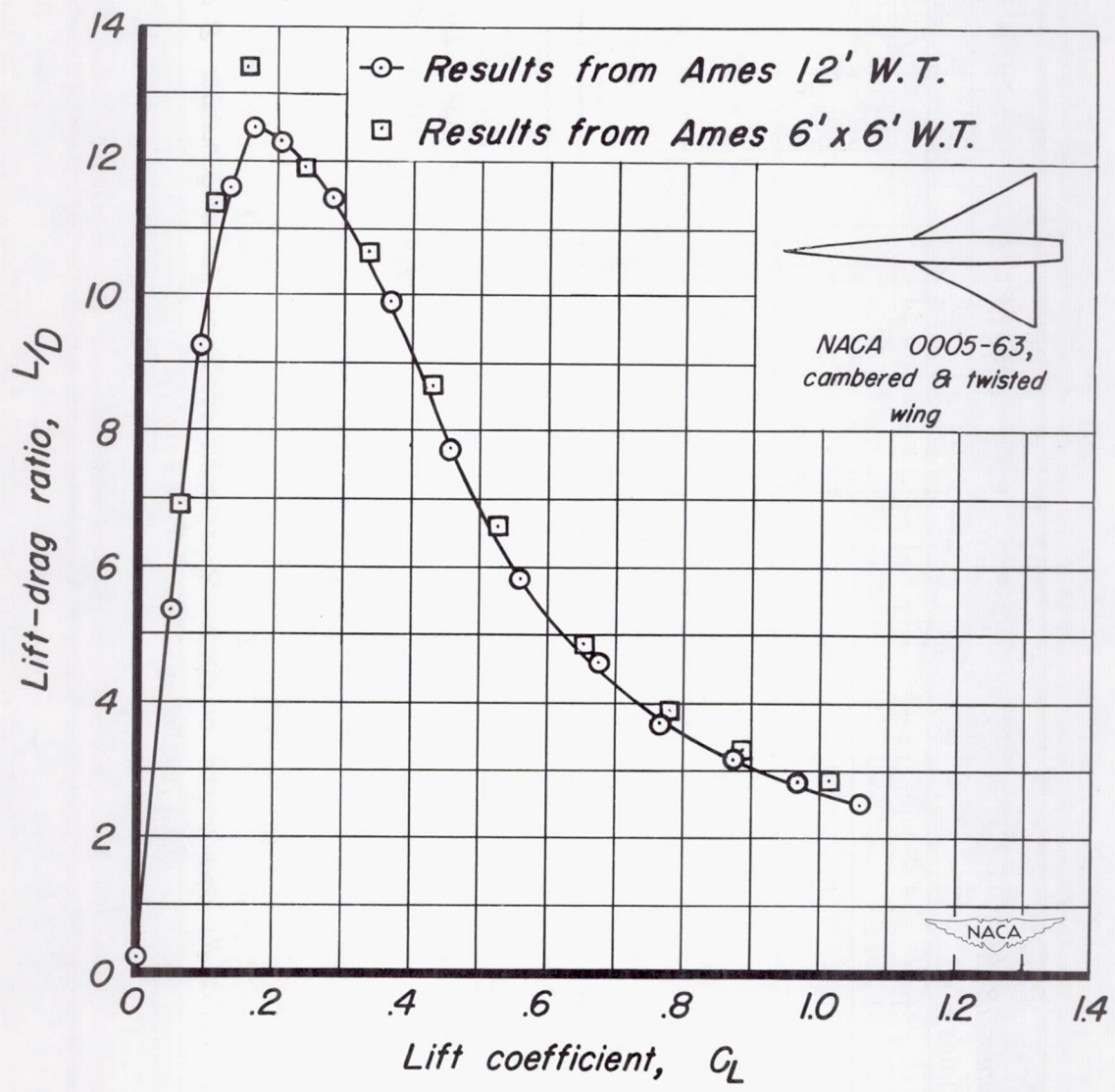
(b) L/D vs C_L

Figure 13.-Concluded.

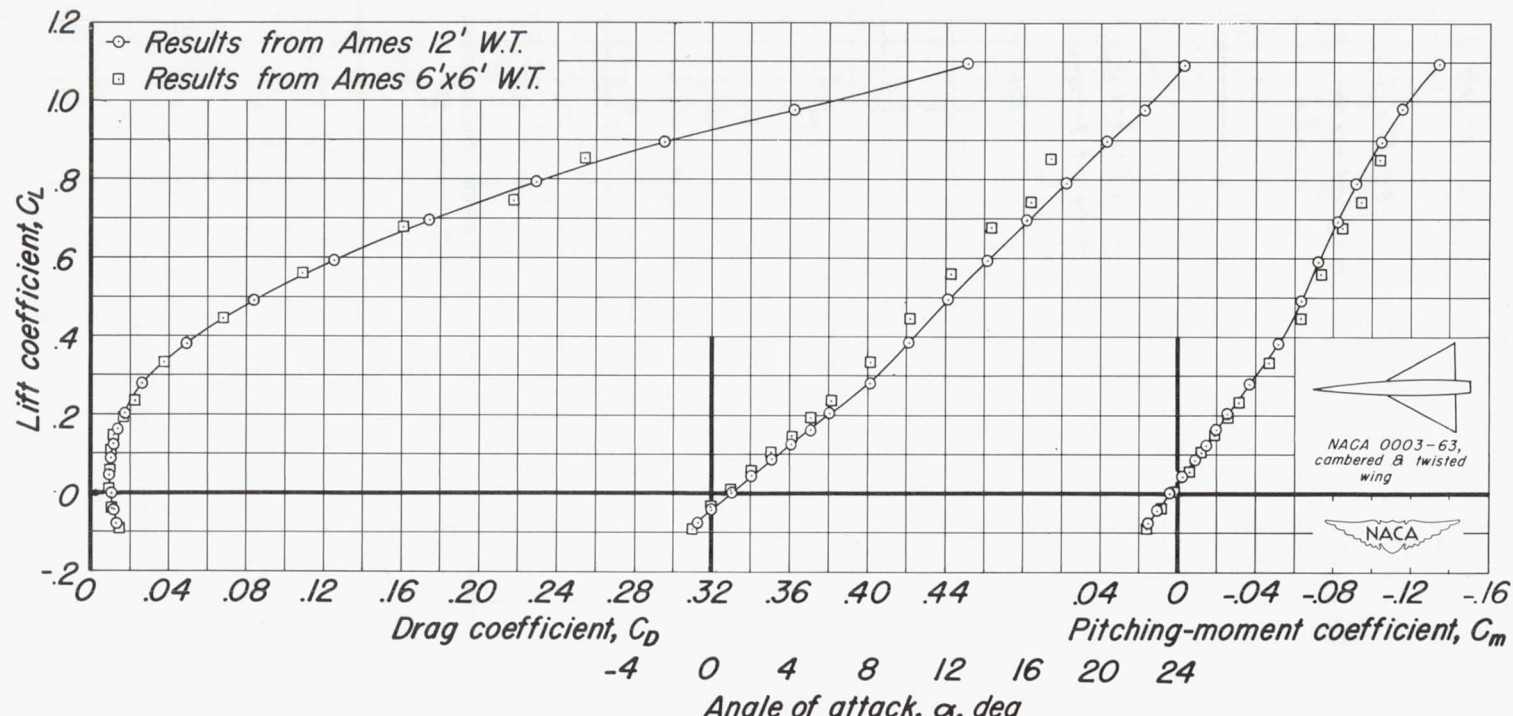
(a) C_L vs C_D , C_L vs α , C_L vs C_m

Figure 14.-The variation of the aerodynamic characteristics with lift coefficient for wing number 3 at a Mach number of 0.60. R , 4.9 million.

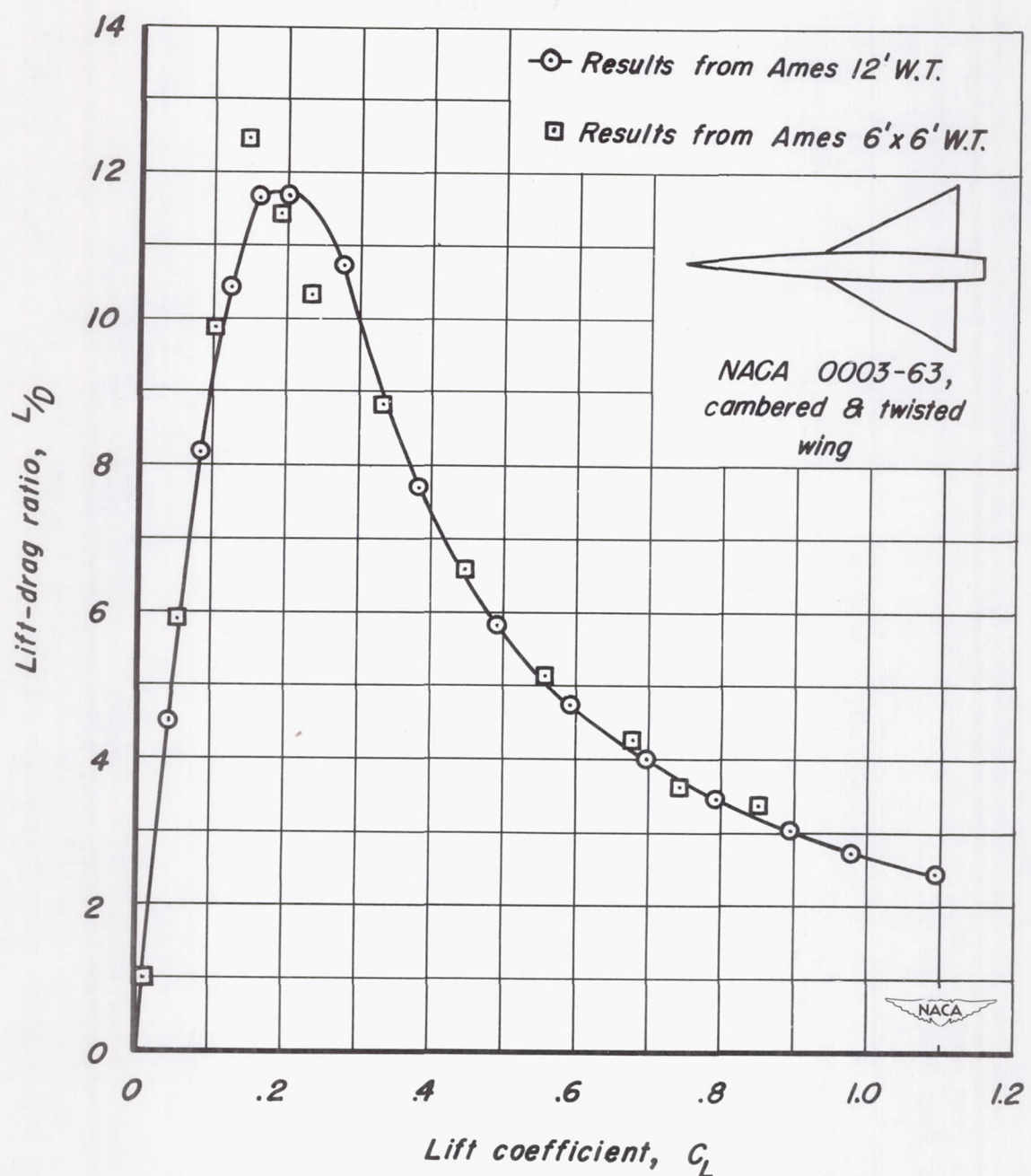
(b) L/D vs C_L

Figure 14.-Concluded.

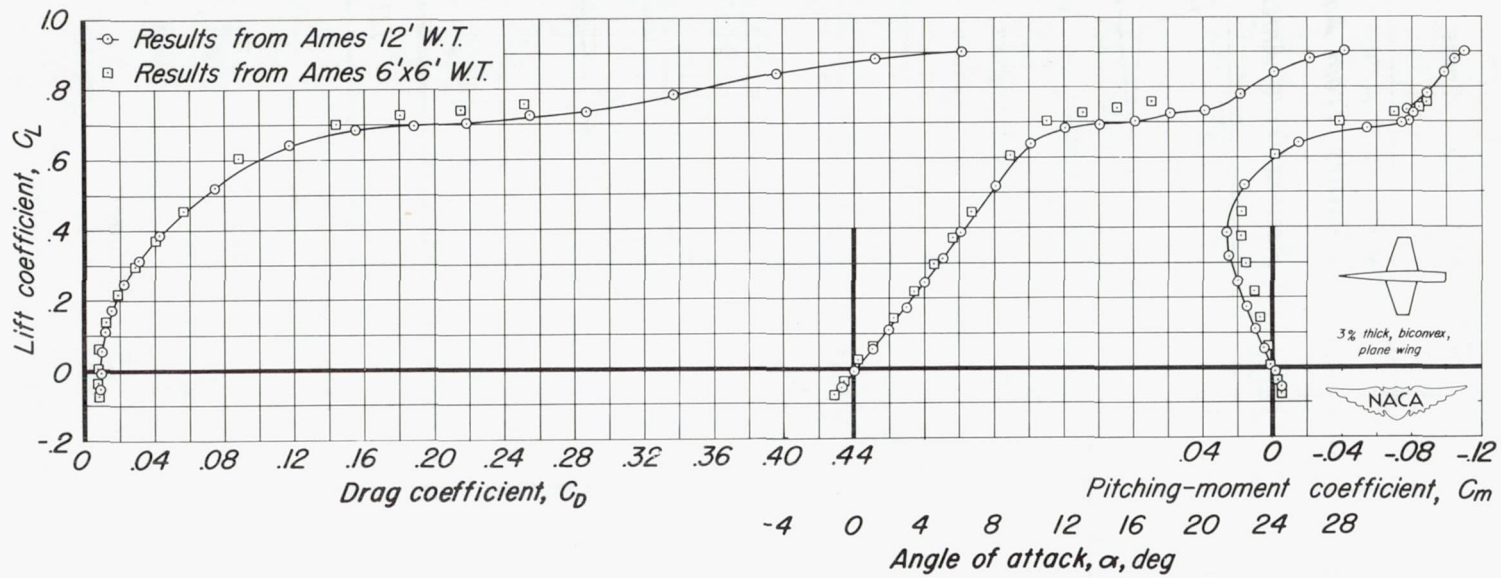
(a) C_L vs C_D , C_L vs α , C_L vs C_m

Figure 15.-The variation of the aerodynamic characteristics with lift coefficient for wing number 4 at a Mach number of 0.60. R, 2.4 million.

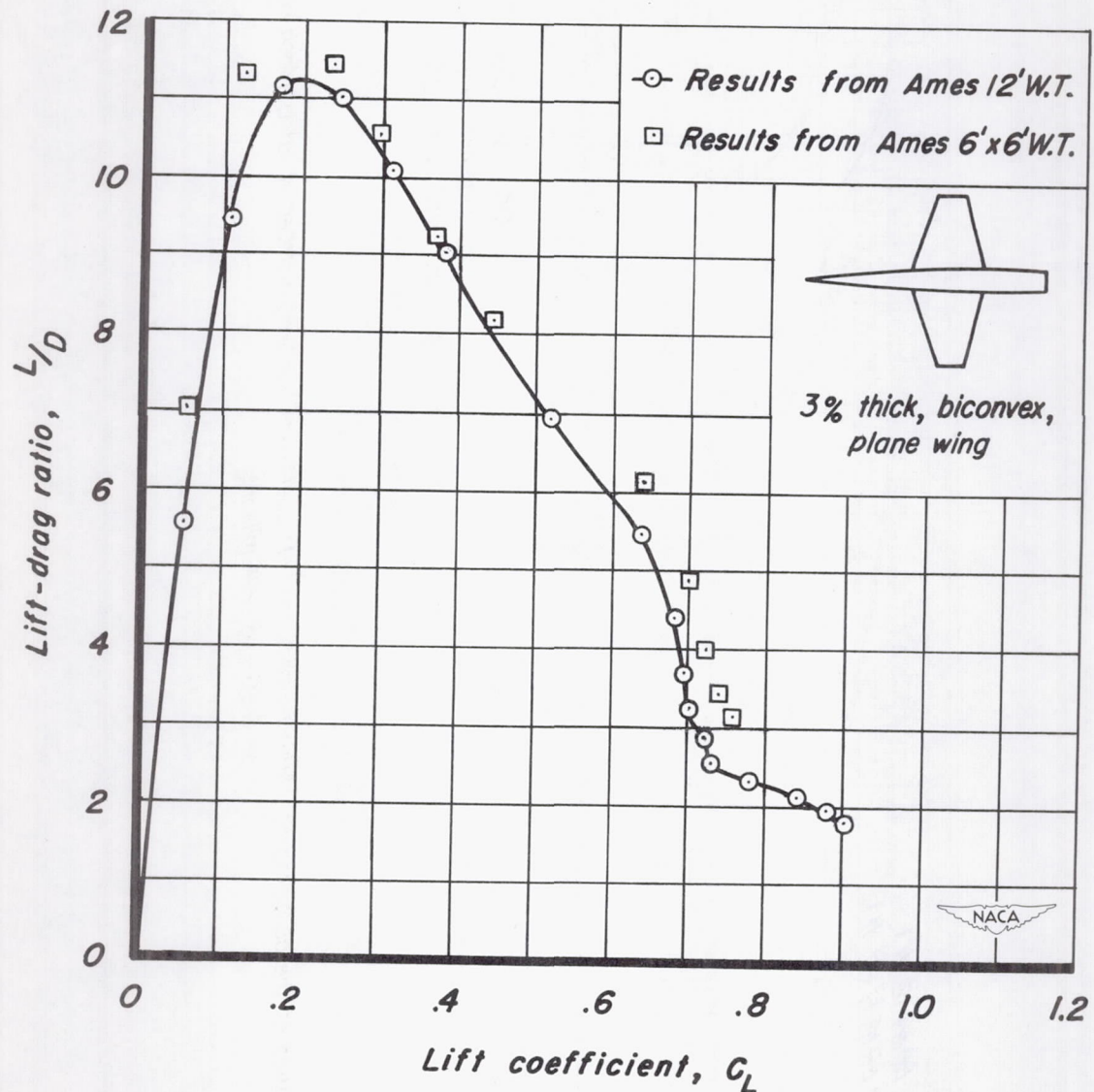
(b) L/D vs C_L

Figure 15.-Concluded.

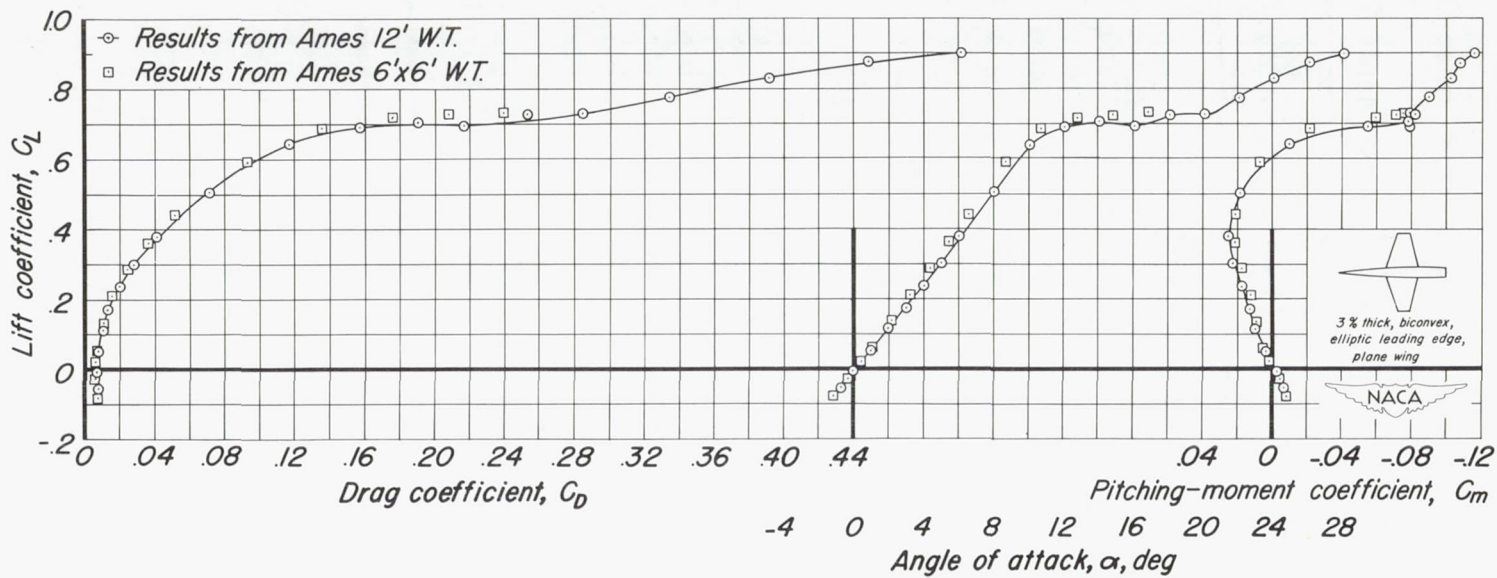
(a) C_L vs C_D , C_L vs α , C_L vs C_m

Figure 16.-The variation of the aerodynamic characteristics with lift coefficient for wing number 5 at a Mach number of 0.60. R , 2.4 million.

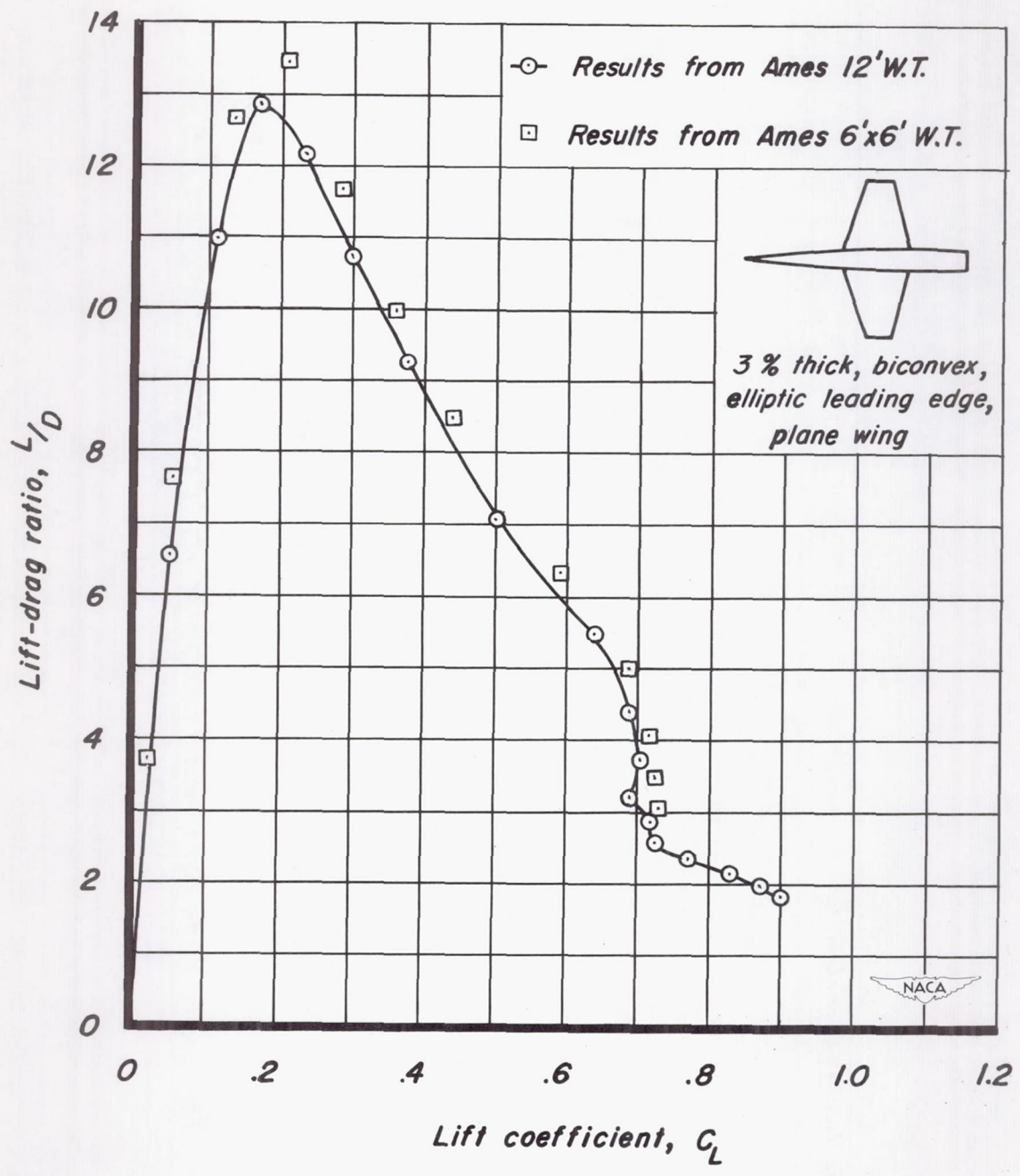
(b) L/D vs C_L

Figure 16.-Concluded.

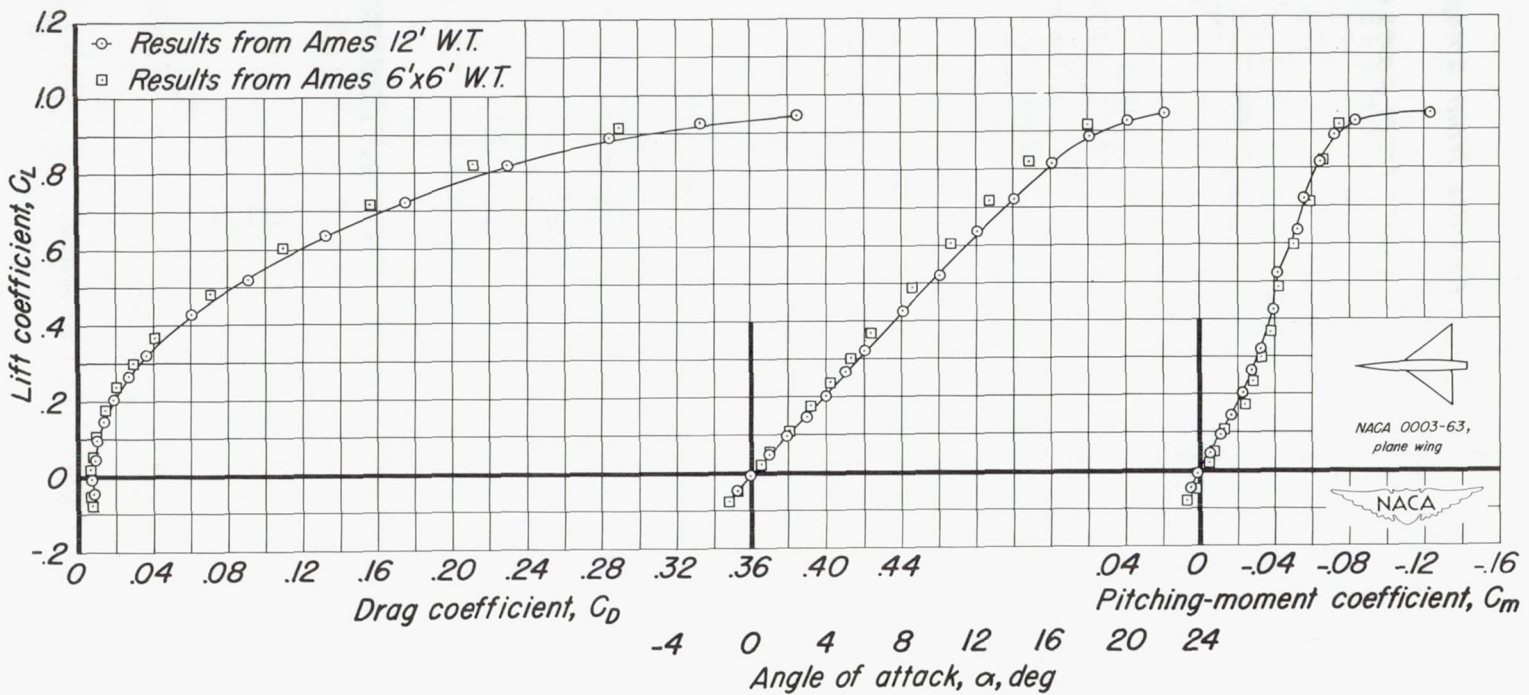
(a) C_L vs C_D , C_L vs α , C_L vs C_m

Figure 17-The variation of the aerodynamic characteristics with lift coefficient for wing number 6 at a Mach number of 0.60. R, 3.1 million.

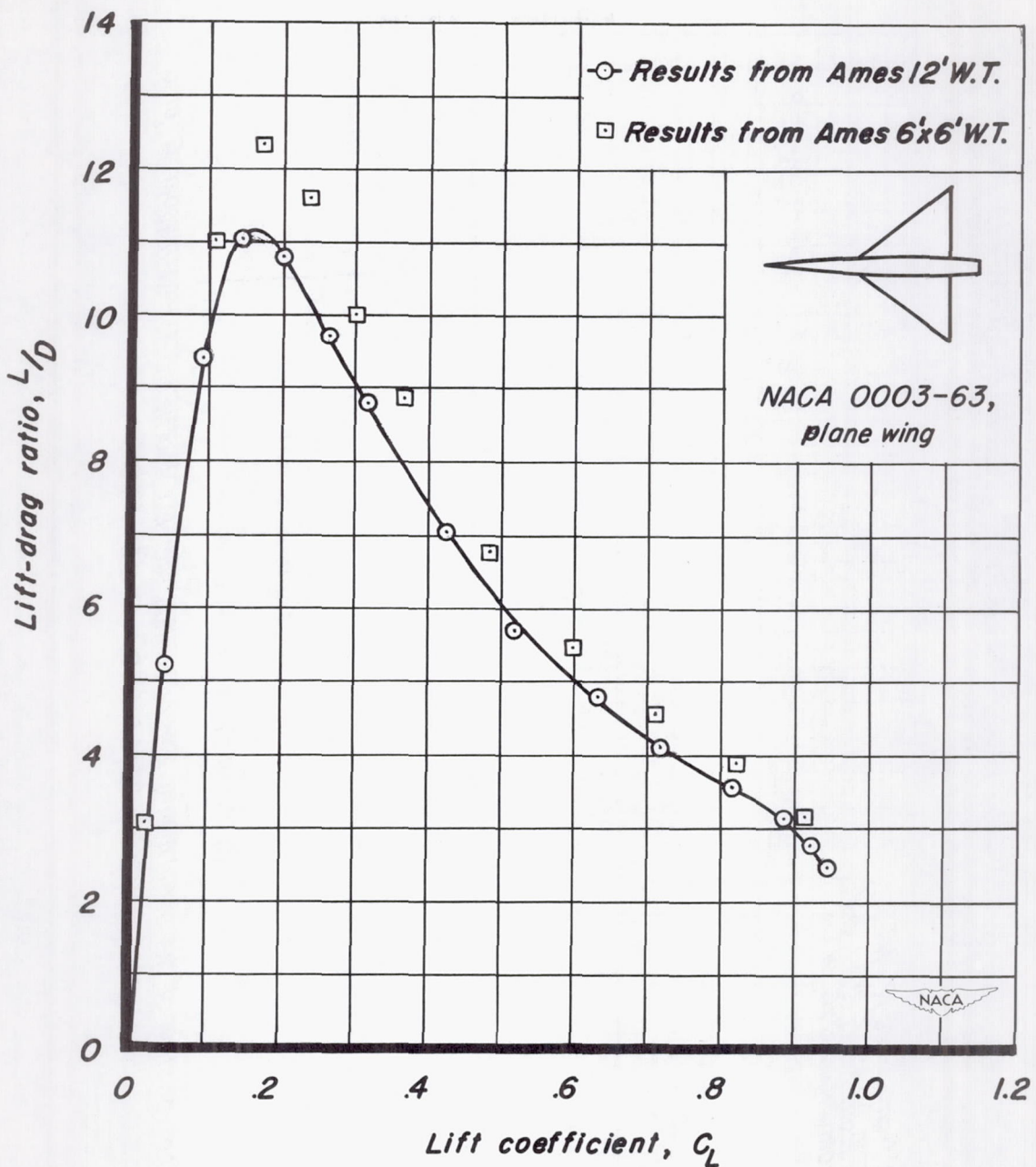
(b) L/D vs C_L

Figure 17-Concluded.

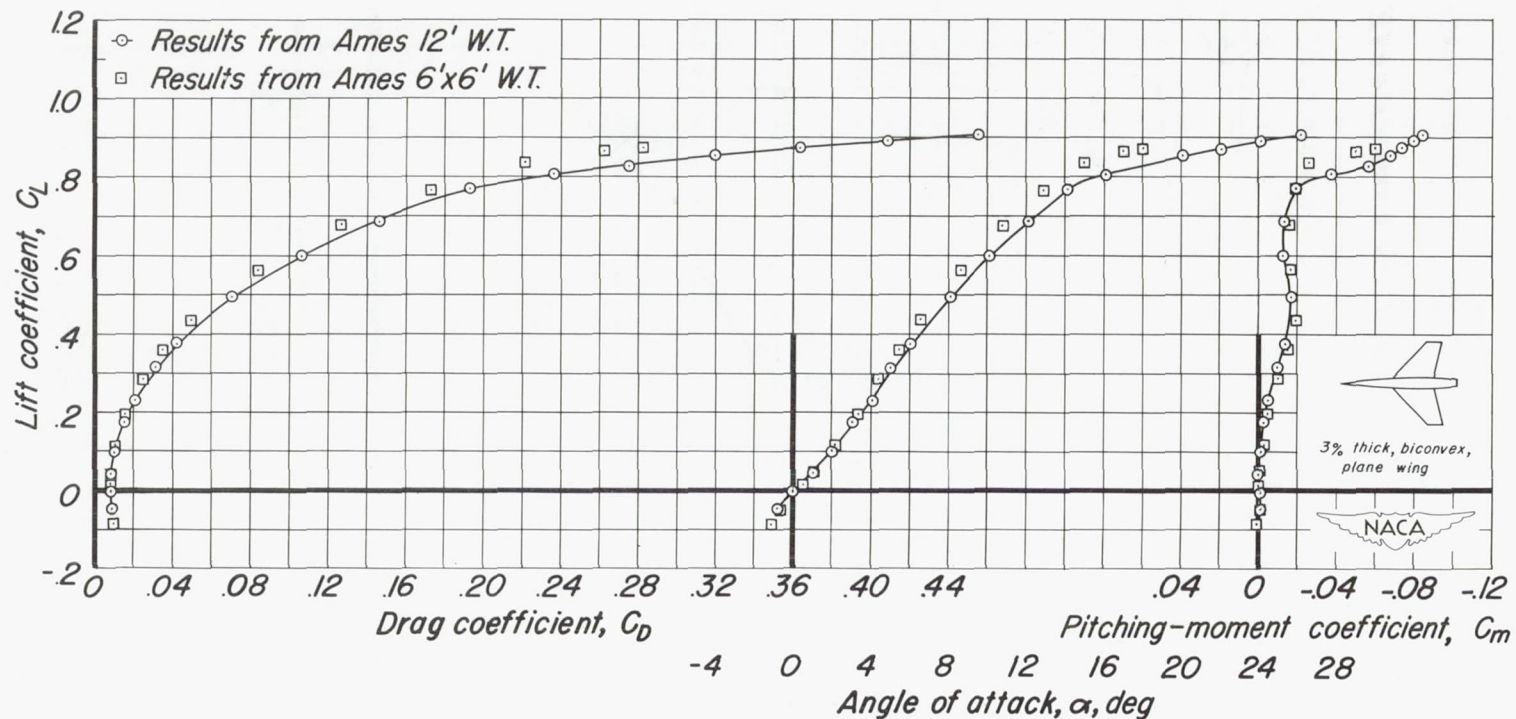
(a) C_L vs C_D , C_L vs α , C_L vs C_m

Figure 18.-The variation of the aerodynamic characteristics with lift coefficient for wing number 7 at a Mach number of 0.60. R, 2.5 million.

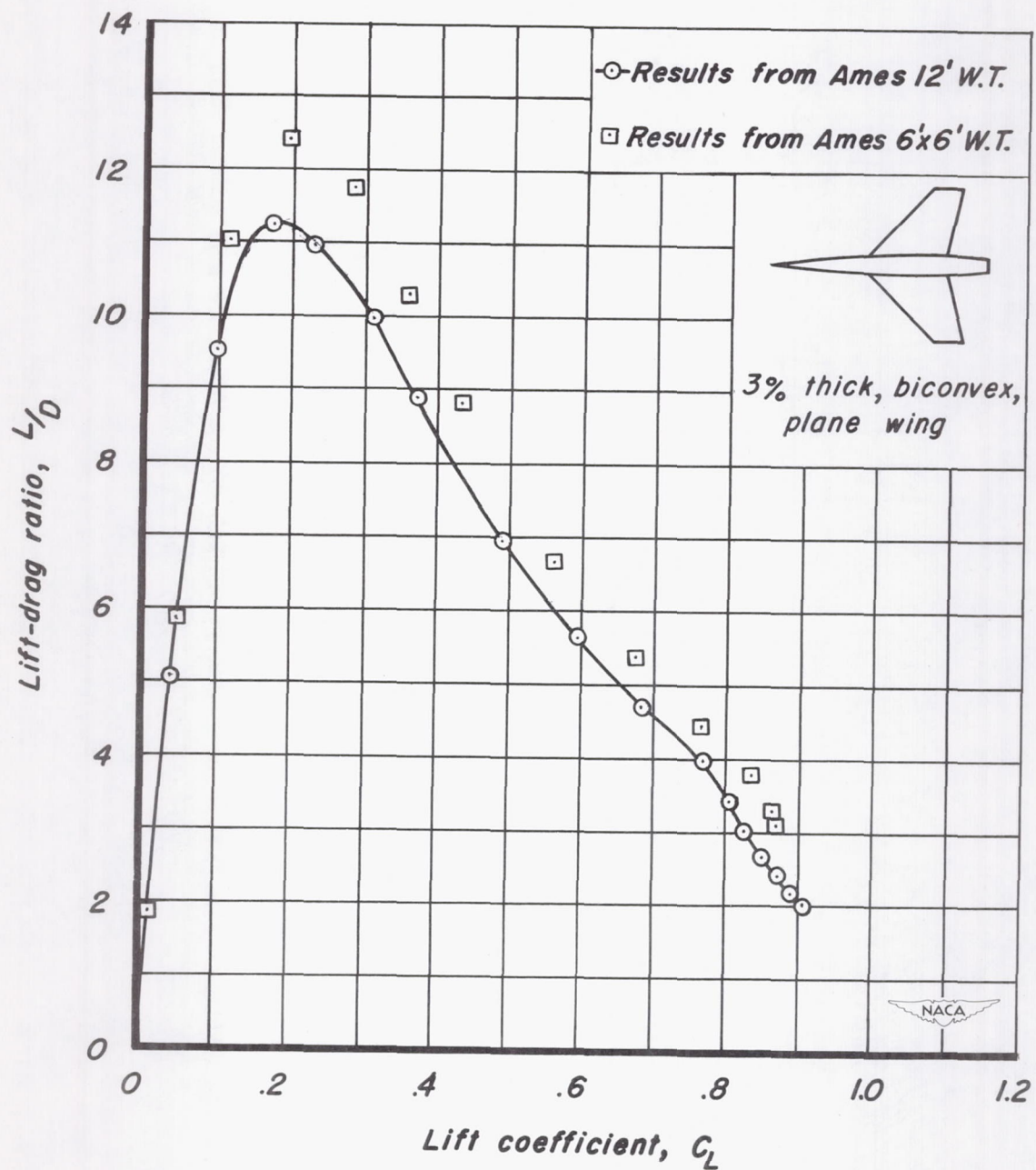
(b) L/D vs C_L

Figure 18.-Concluded.

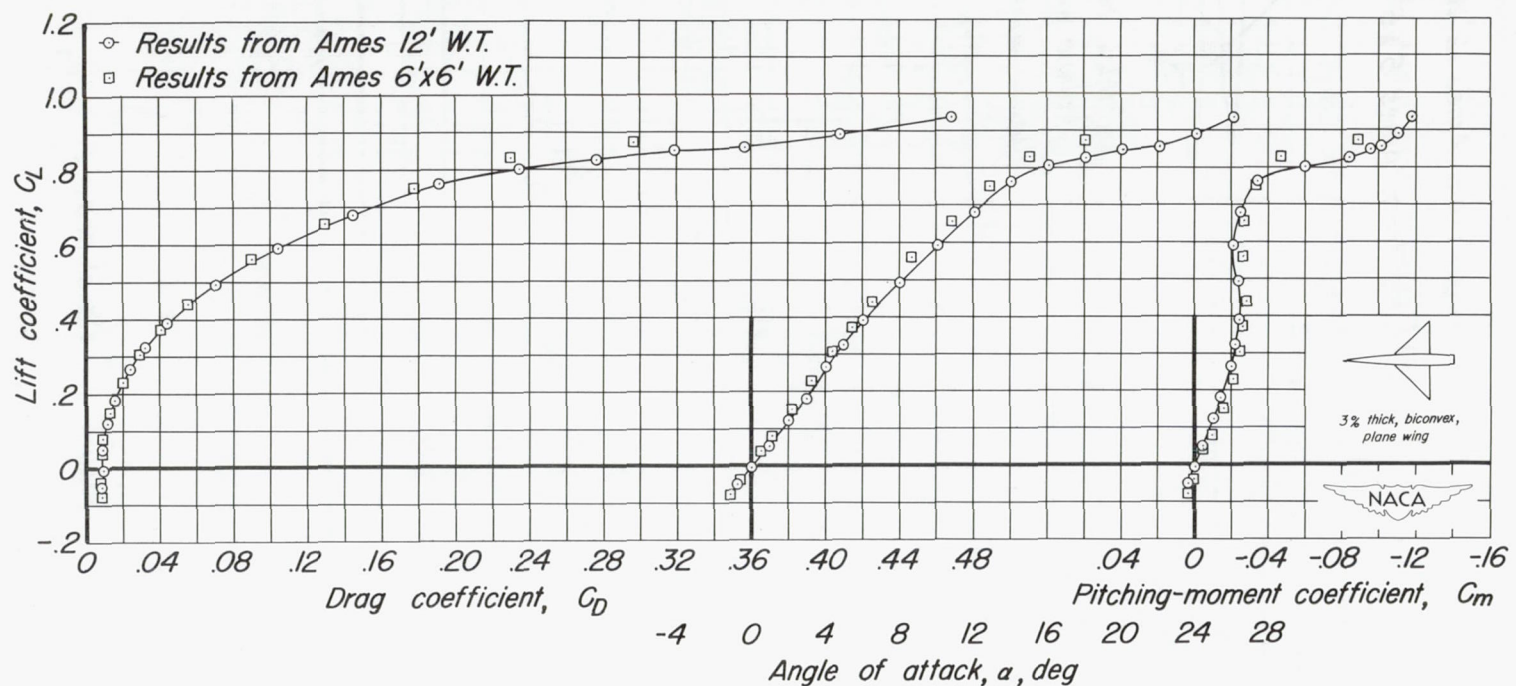
(a) C_L vs C_D , C_L vs α , C_L vs C_m

Figure 19.-The variation of the aerodynamic characteristics with lift coefficient for wing number 8 at a Mach number of 0.60. R , 2.7 million.

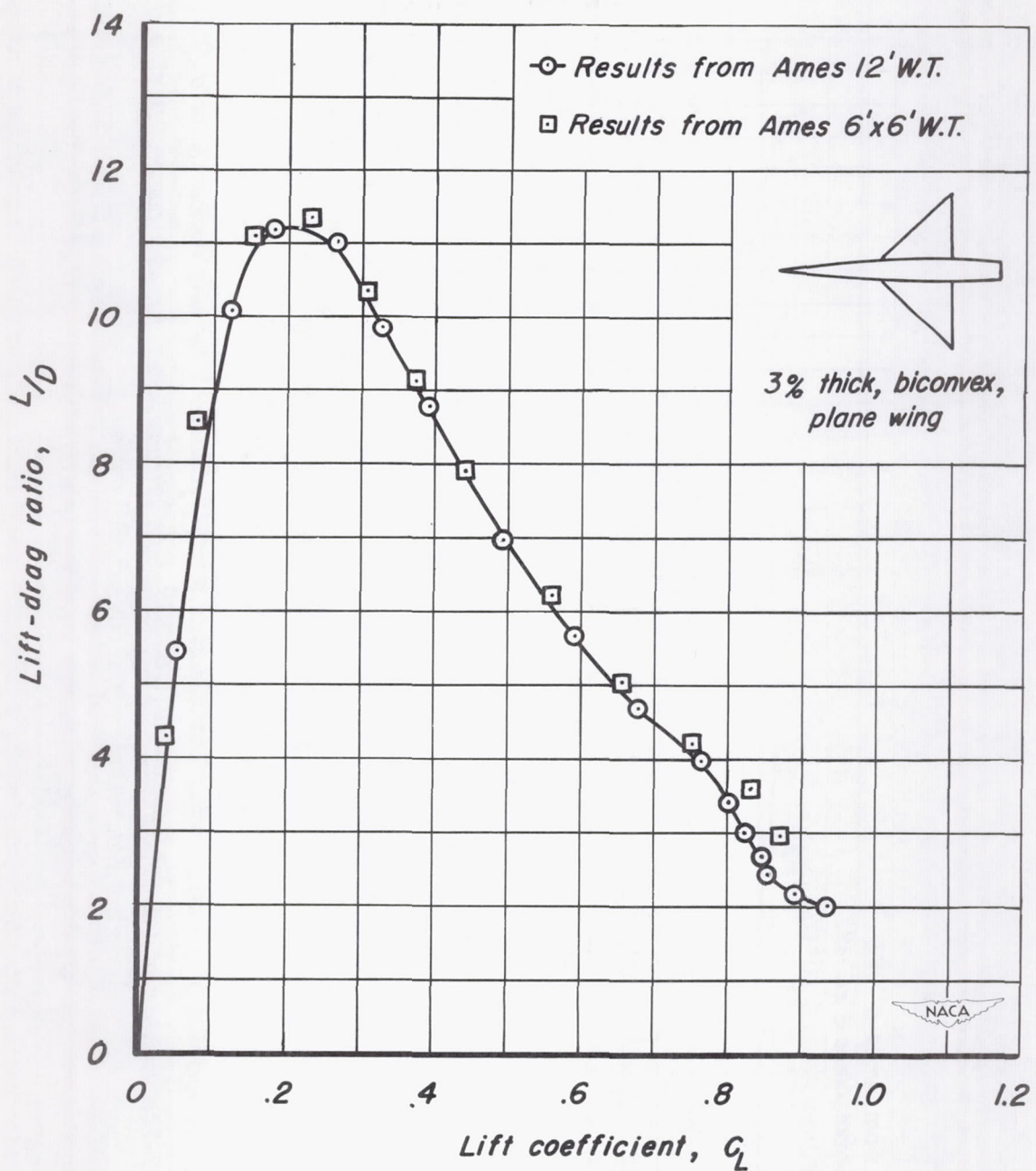
(b) L/D vs C_L

Figure 19-Concluded.

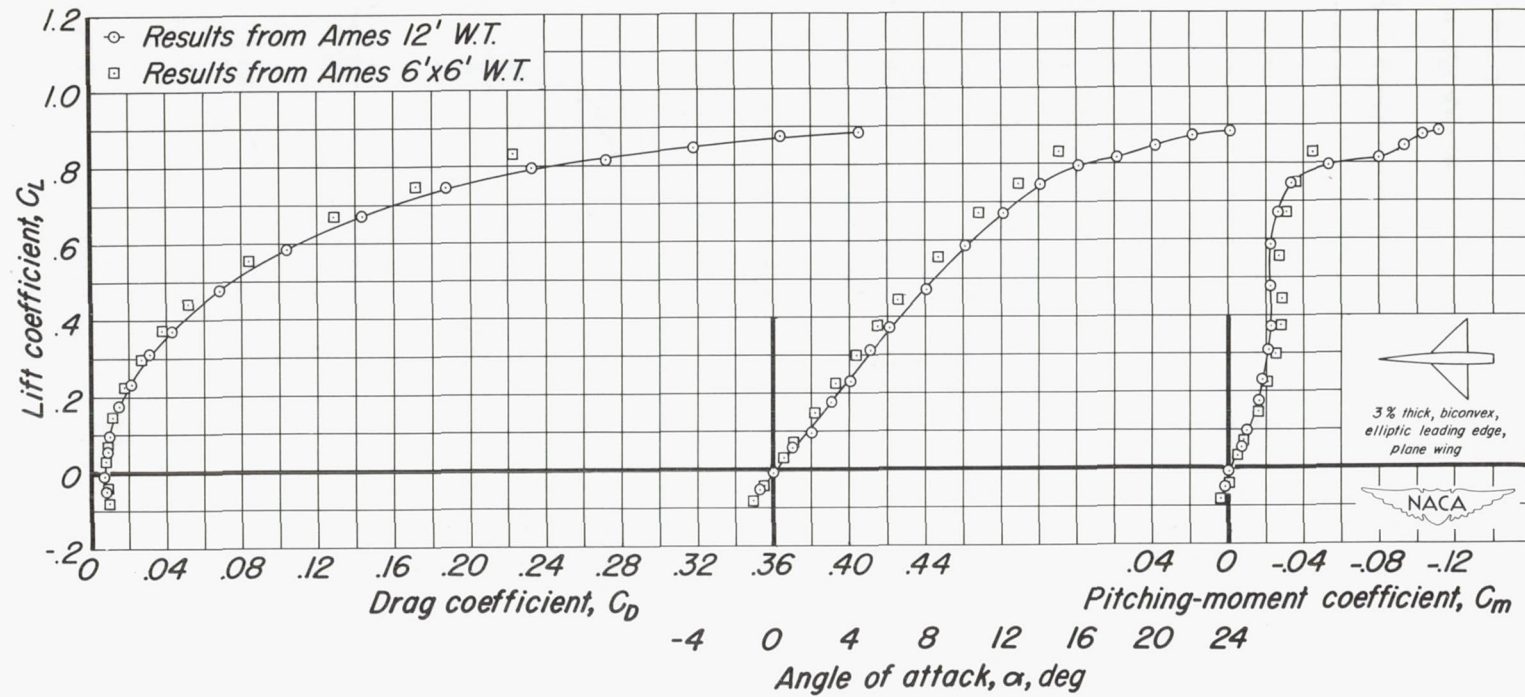
(a) C_L vs C_D , C_L vs α , C_L vs C_m

Figure 20.-The variation of the aerodynamic characteristics with lift coefficient for wing number 9 at a Mach number of 0.60. $R, 2.7$ million.

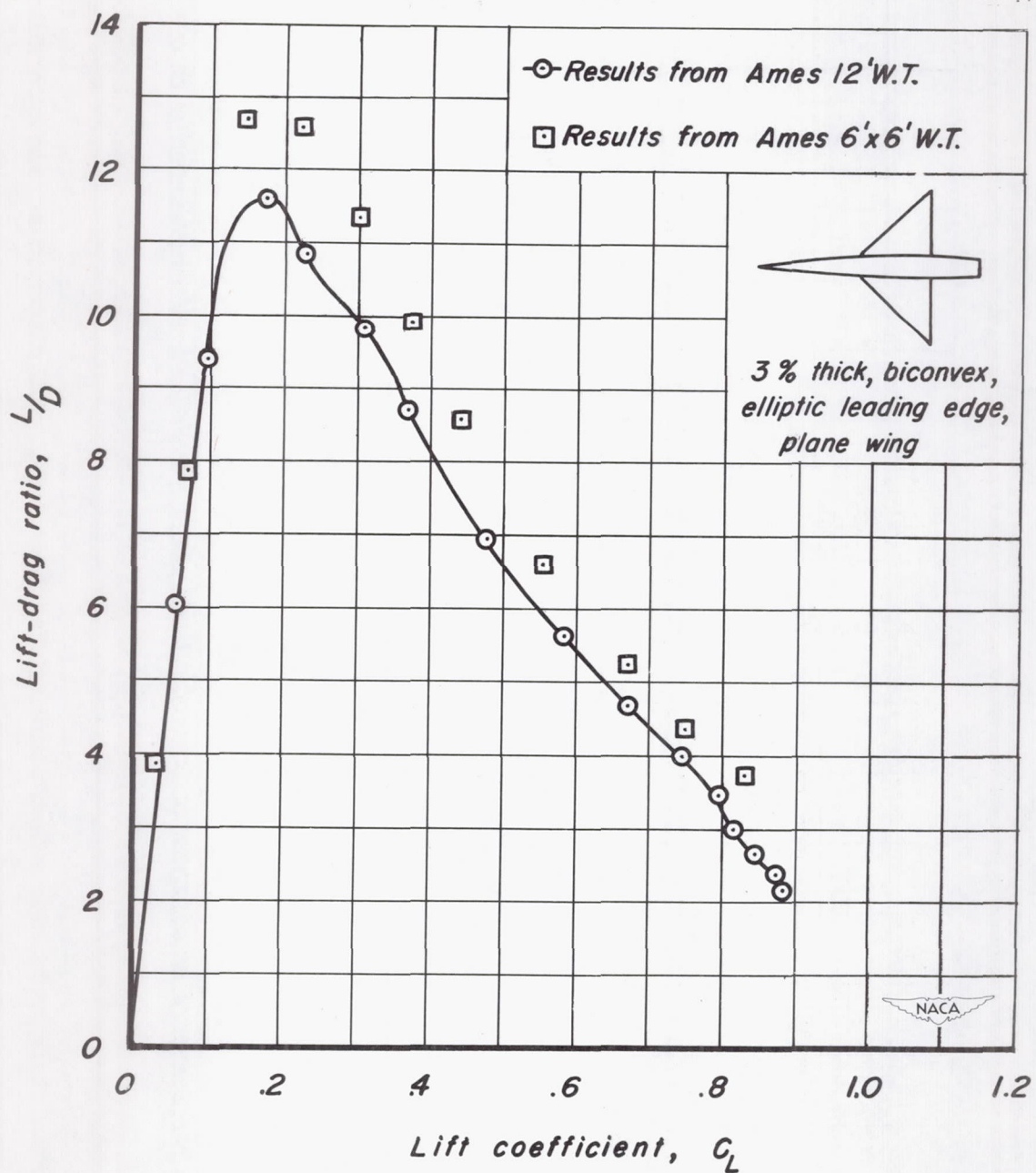
(b) L/D vs C_L

Figure 20.-Concluded.

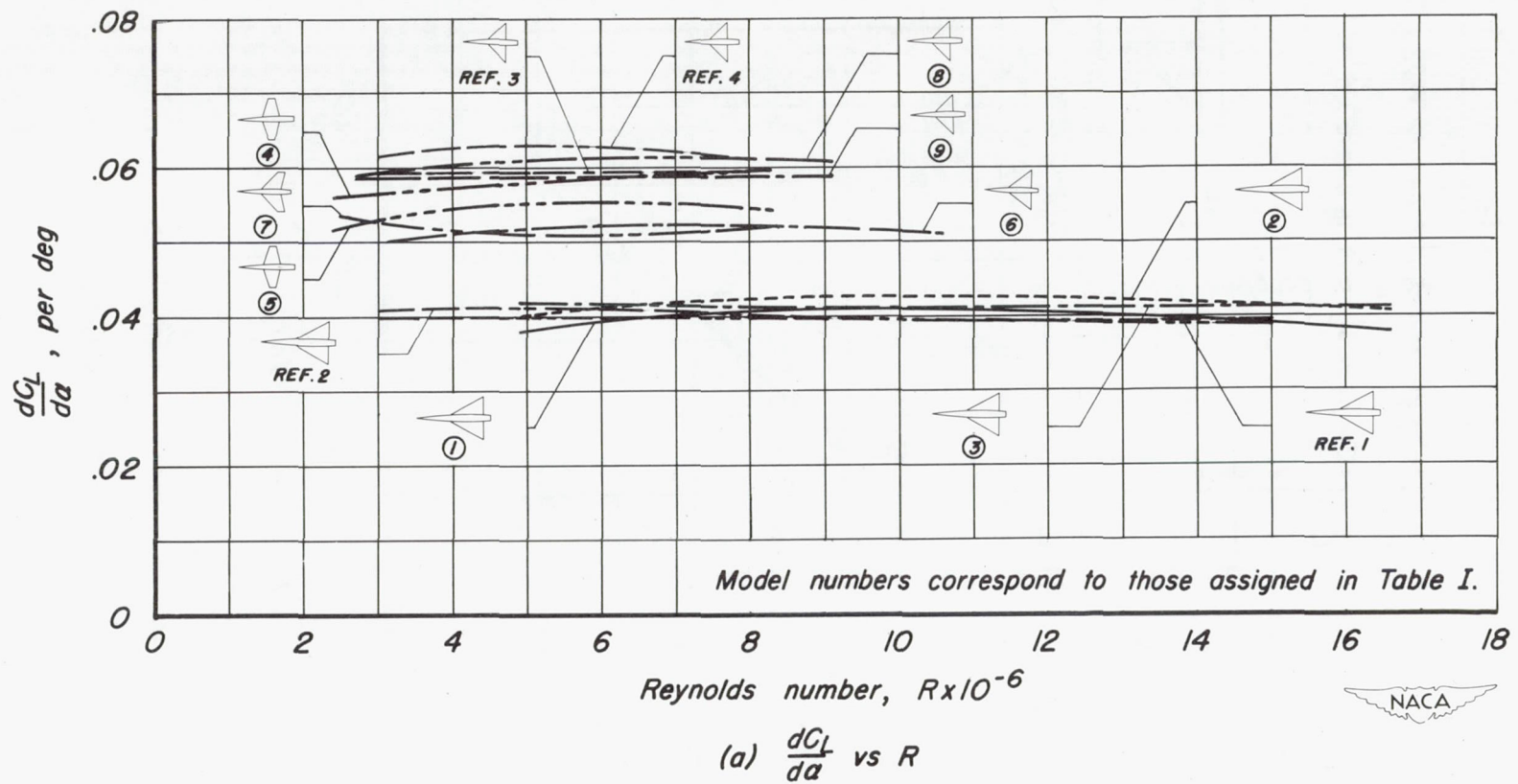


Figure 21.—Summary of aerodynamic characteristics as a function of Reynolds number. $M, 0.25$.

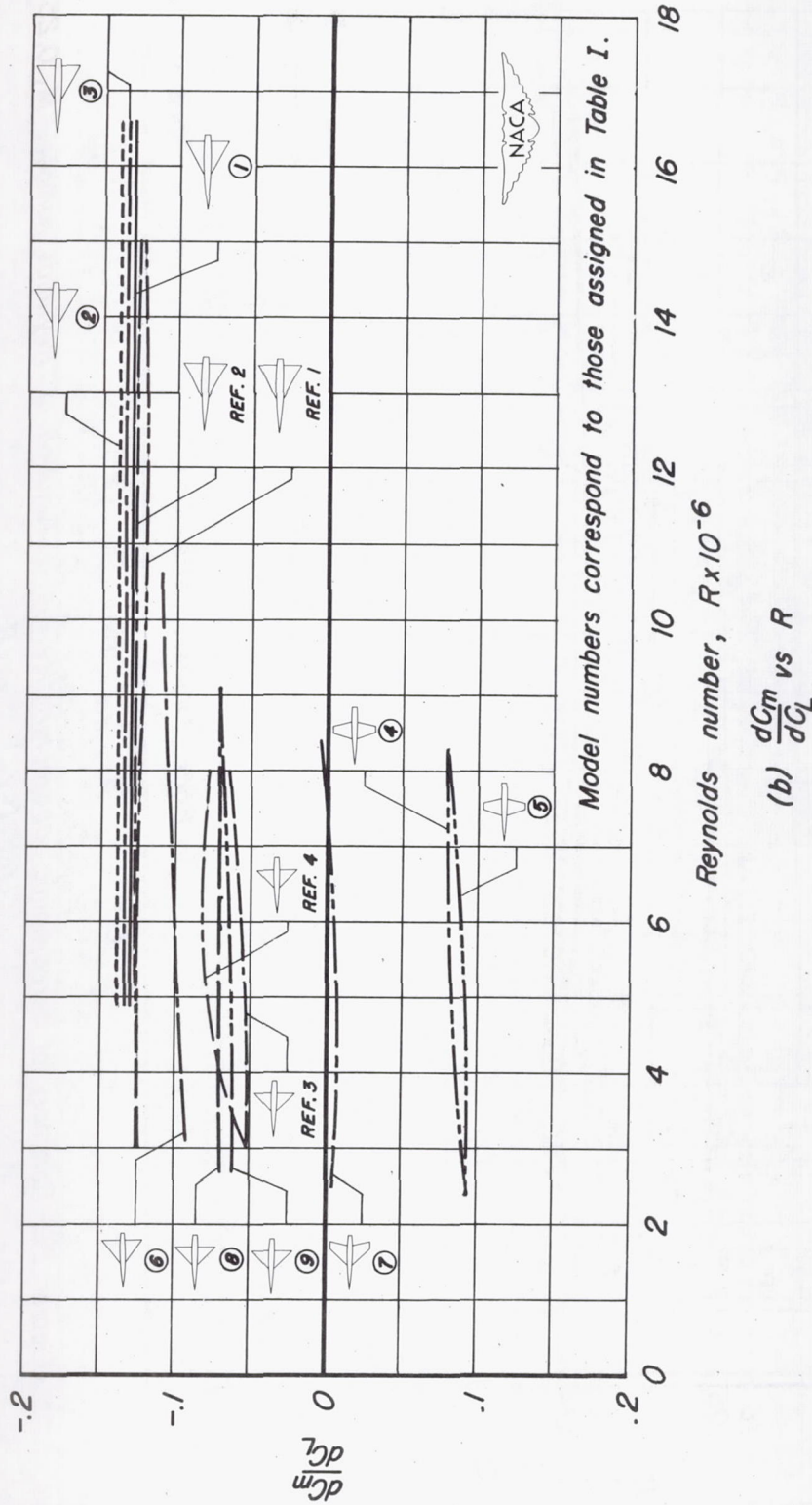


Figure 21.-Continued.

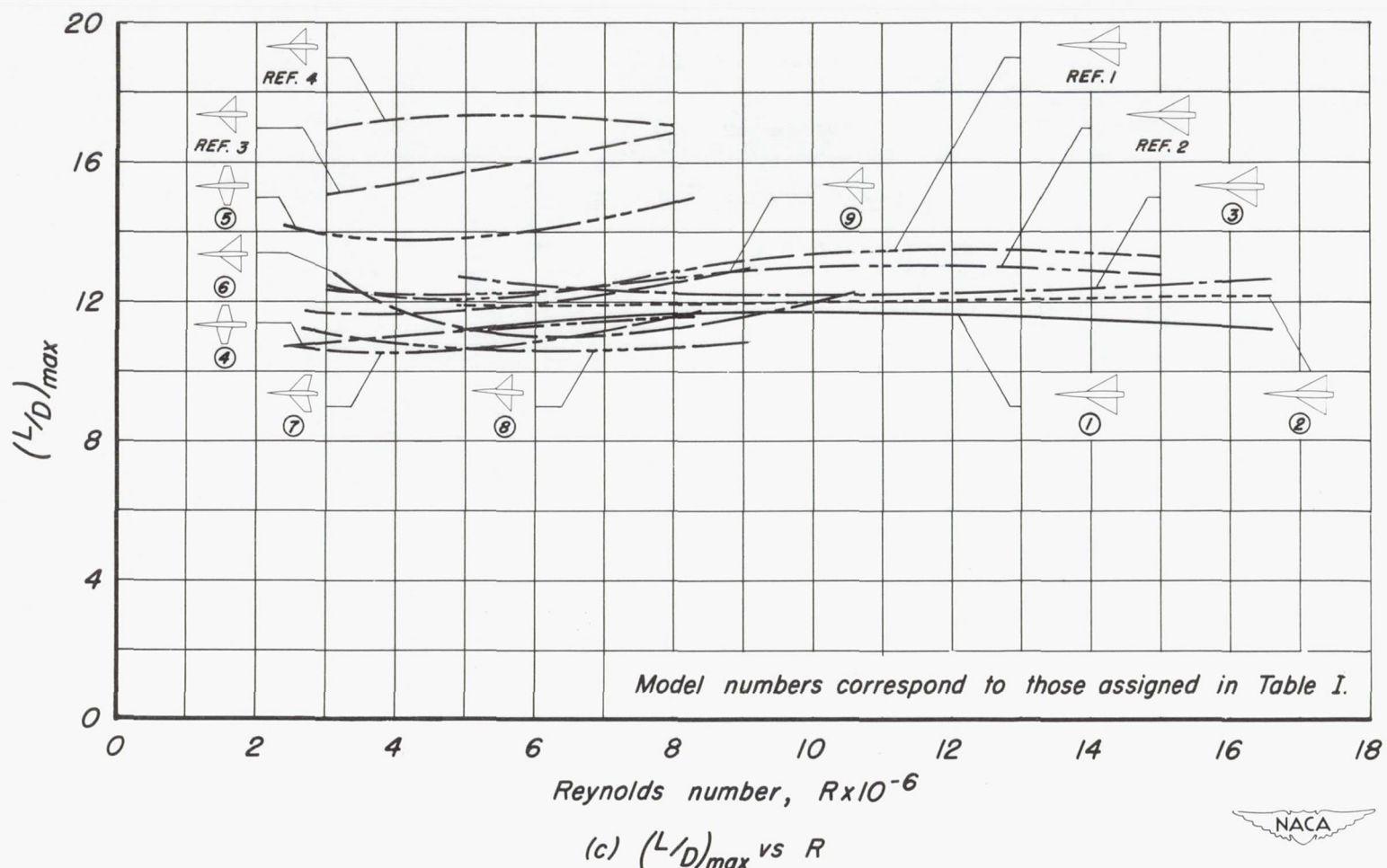


Figure 21.-Continued.



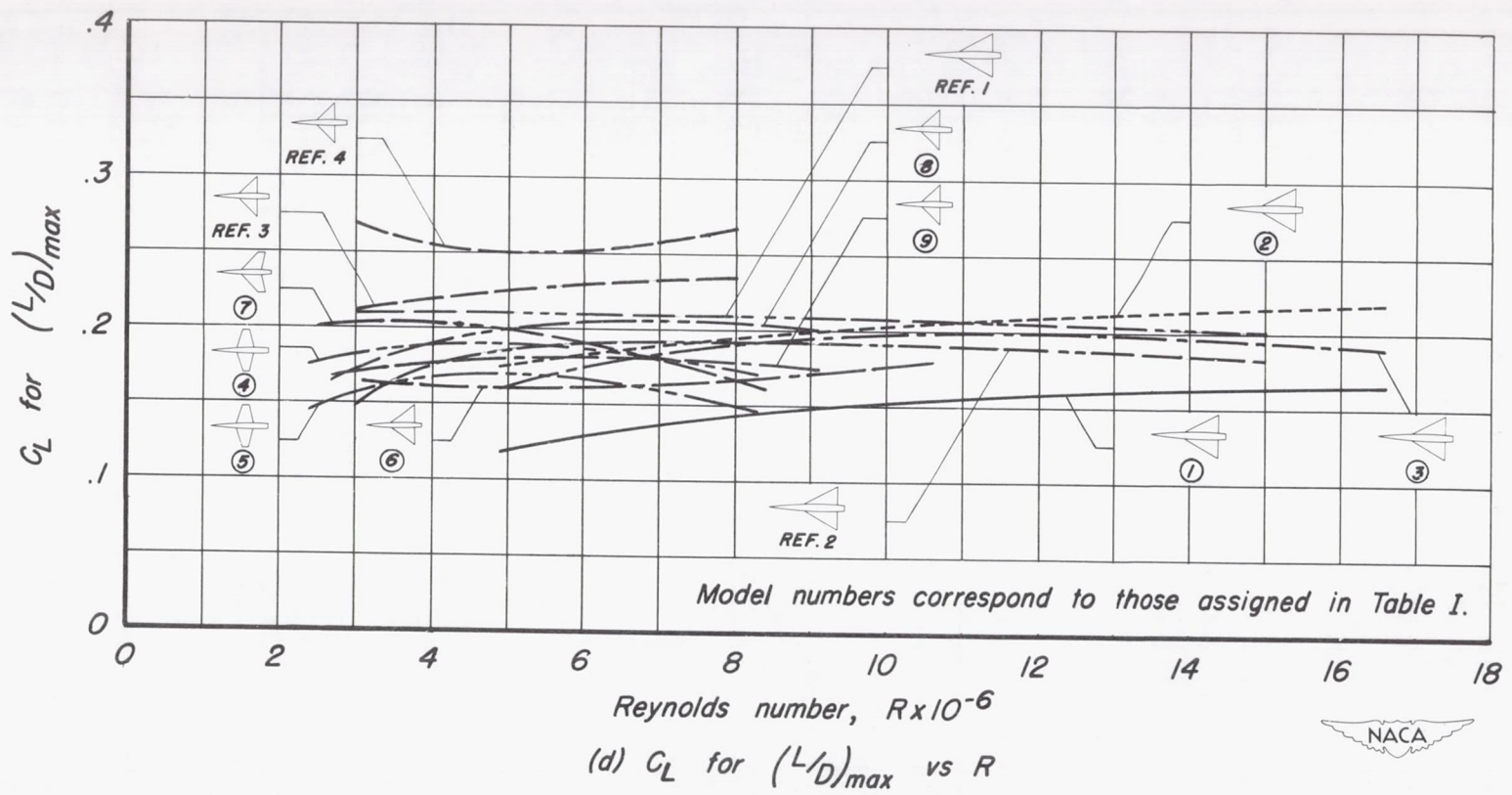
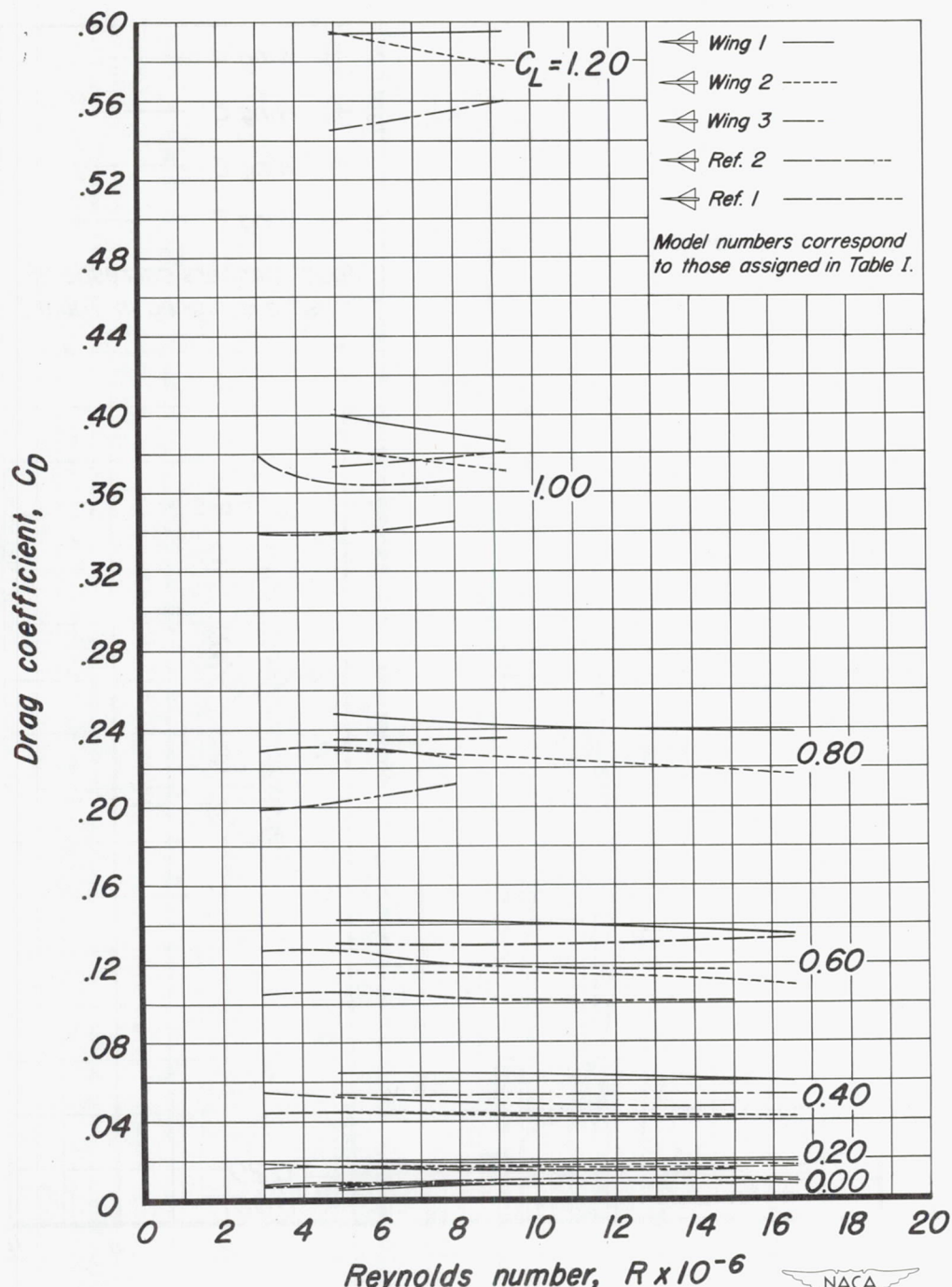


Figure 21.-Concluded.





(a) Aspect ratio, 2.0



Figure 22 -A summary of the variation of drag coefficient with Reynolds number at several lift coefficients. $M, 0.25$.

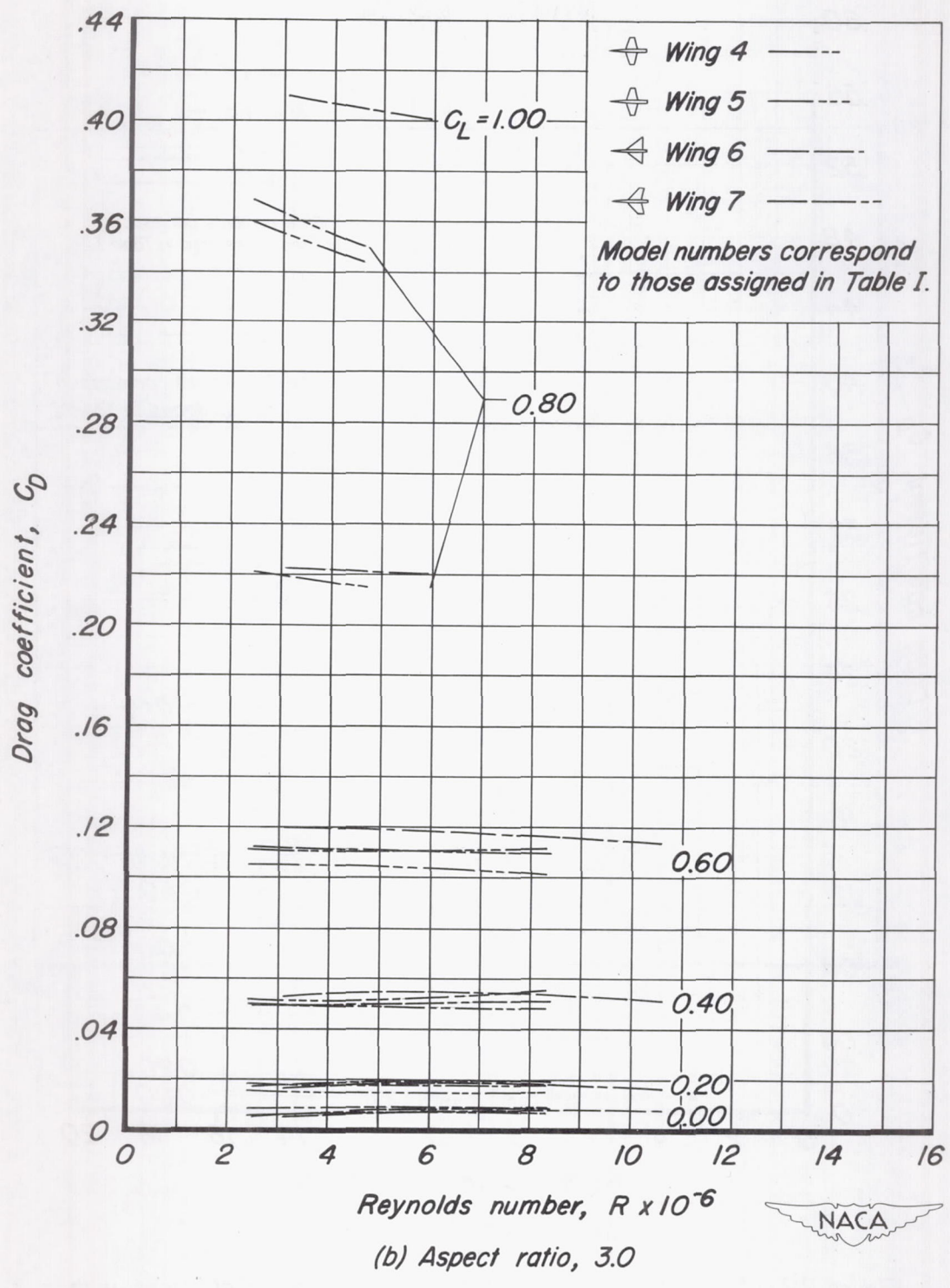
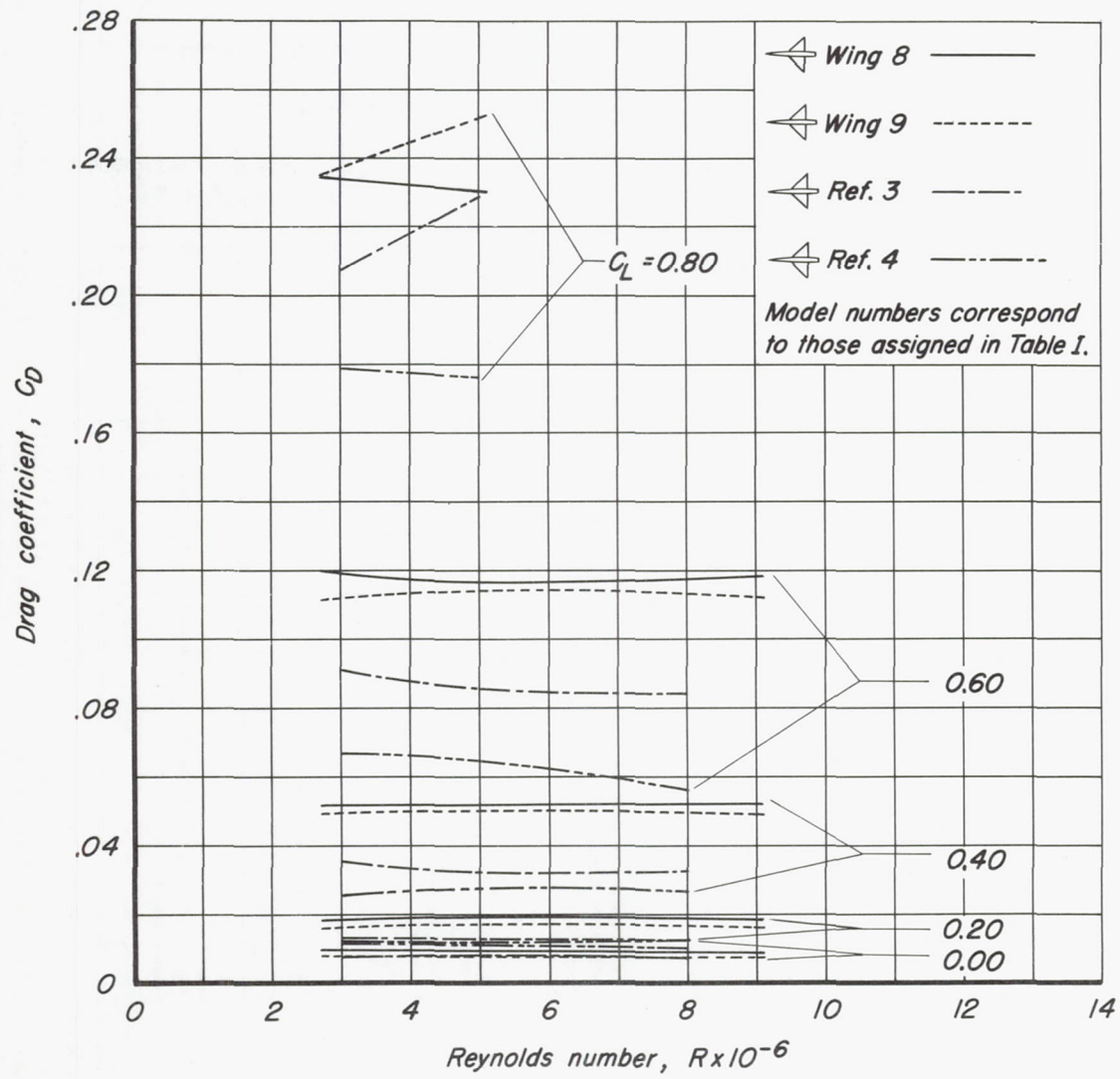


Figure 22.-Continued.



(c) Aspect ratio, 4.0



Figure 22.-Concluded.